ENEA – Progetto CERSE
Dipartimento di Meccanica & Aeronautica – Gruppo CIRCUS

TR ENEA/DMA/010509
Final Report

May 7, 2009

Enrico Sciubba

FOREWORD

One of the critical areas of the IGCC technology is the sulfur removal from the syngas. Current processes are of the "cold" type: the syngas is cooled downstream of the gasifier, treated, and then reheated before combustion: this is scarcely an optimal procedure, and leads in fact to an important loss of global efficiency. A promising alternative is the HTHPD, a high-temperature/high-pressure desulfuration process based on a regenerable Zn/Ti sorbent. In the HTHPD the sulfur compounds are first adsorbed in a fluidized-bed reactor by sorbent pellets that are then transported to another reactor to be regenerated in an O_2-rich stream: the sulfur is removed as SO_2 or $CaSO_4$. At present, the HTHPD technology is at pilot-scale demonstration stage, and the first results show a potential for improving the overall plant efficiency by about one percentage point.

The Project ENEA/DMA foresaw the development of a physical-chemical model of a HTHPD device and its implementation in a simulation environment consisting of a modular process simulation software (CAMEL-Pro) that allows the user to solve and analyze plant configurations by using components and streams previously defined in the code's libraries.

In the work performed within the scope of the present project, we have modeled a high-temperature/high-pressure desulfuration process (HTHPD) that employs a regenerable Zn/Ti based sorbent. The model is based on strongly simplified reaction kinetics, on a proper black-box schematization of the known phenomenological aspects of the problem, on published data about process schemes and on the few available experimental results.

The desulfuration reactor model relates the reactor performance with the sorbent characteristics and the operating conditions: temperature, pressure, syngas mass flow, H_2S concentration, etc., deriving real-scale reactor results from lab-scale experimental results. The performance curves obtained for the HTHPD do not make explicit use of reaction kinetics, but in a way "embed" it in an integral sense, in the same way a compressor operating map "embeds" the local thermo-fluiddynamics of the flow.

As such, the general method described in this Report can be used to derive the performance maps of any chemical reactor, paving the way to a series of practical applications in the development of process simulators.

MODELING, SIMULATION AND OPTIMIZATION OF A SYNGAS DESULFURIZATION DEVICE

ABSTRACT

This report discusses the flue gas desulfurization process in general and syngas desulfurization in particular. It presents the fundamental and practical aspects of the current available technology and provides an overview of the strengths and limitations of different technologies.

This study is part of a larger research project in progress at the Department of Mechanical and Aeronautical Engineering of the University of Rome 1, "La Sapienza": the analysis and simulation of a hydrogen-fed steam power plant based on the ZECOTECH© cycle in which an H_2-rich syngas is produced by a strongly integrated coal gasification and CO_2 capture process. Therefore, the present study is strongly biased towards desulfurization methods suitable for the chemical section of this plant.

Current commercial desulfurization processes need to operate on a cool gas to be effective, typically at 40ºC. Since the syngas is produced in reactors that are maintained at high temperature and pressure, the development of a process that allows for the elimination of the sulfur compounds without requiring preliminary stages of cooling and depressurization leads to an important reduction of the irreversibility of the procedure.

The modeling and simulation is performed by using CAMEL (CAlculation by Modular ELements), a code simulator for thermal processes that has been conceived and implemented by the Mechanical and Aeronautical Department of the University of Roma 1, "La Sapienza". CAMEL allows the user to solve and analyze plants configurations that have been properly assembled by using components and streams previously defined in the code's libraries.
This work describes the development of a new component and its insertion into the CAMEL library. In this particular case, we study a desulfurization device.

This report is significant in that in reports a comprehensive study of the modeling, simulation and optimization of a syngas desulfurization device integrated in a "zero CO_2 emissions" coal gasification process. The code, enhanced with the routines developed herein allows for a more complete and accurate simulation of the hydrogen-fed steam power plant, including the process of syngas desulfurization.

TABLE OF CONTENTS

This section describes the link between the intensive utilization of the combustion fossils and the large scale climatic changes, which is presently one of the greatest challenges faced by our species. We summarize some short and medium range strategies that have been proposed as a possible alternative to fossil fuels, and describe where this research can fit in the scenarios they delineate. Finallyly, we give an overview of the approach used in this study.

1.1 Climatic Change

The correlation between human activities and the rapid climatic changes the planet has undergone in the last century has been made clear by several scientific studies [1.1].
Especially appalling is the global warming effect of the increasing concentrations of atmospheric greenhouse gases, such as carbon dioxide (CO_2), methane (CH_4), and nitrous oxide (N_2O).
Simply explained, a portion of the infrared radiaton emitted by the Earth's surface is partially absorbed in the atmosphere by greenhouse gases and clouds, and leads to a decrease of the radiating back-radiation of the Earth into space (greenhouse effect). In the industrial era, human activity, primarily the uncontrolled burning of fossil fuels, have added greenhouse gases to the atmosphere, which have greatly intensified the natural greenhouse effect, exasperating the warming of Earth's climate.
The Intergovernmental Panel on Climate Change (IPCC) reports [1.1] offer exhaustive data and evidence, result of extensive scientific work, to support this statement. The most significant information can be found in the two following figures:

- Figure 1.1 displays records of past changes in atmospheric concentration of CO_2, CH_4 and NO_2 to provide context for the influence of anthropogenic emissions. The records confirm the large growth in emissions derived from human activity during the Industrial Era.

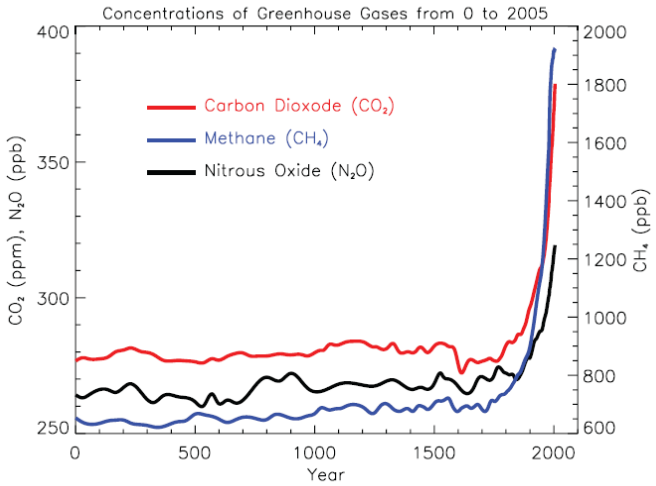

Figure 1.1: Atmospheric concentrations of important long-lived greenhouse gases over the last 2,000 years [1.1]

Anthropogenic carbon dioxide emissions come from fossil fuel use in transportation, space conditioning and industry. Apart from industrial emissions, Methane has increased as a result of intensive agricultural practices, natural gas distribution and landfills. Nitrous oxide is also emitted by human activities such as fertilizer use and fossil fuel burning.

- Figure 1.2 shows the annual global mean observed temperatures (black dots) and some simple linear fits. The left hand axis shows anomalies relative to the 1961 to 1990 average and the right hand axis shows the estimated actual temperature (°C). Linear trend fits to the last 25 (yellow), 50 (orange), 100 (purple) and 150 years (red) are shown, and correspond to 1981 to 2005, 1956 to 2005, 1906 to 2005, and 1856 to 2005, respectively. Note that for the more recent periods the slope is higher, indicating accelerated warming. The blue curve is a smoothed depiction to capture the decadal variations. To give an idea of whether the fluctuations are meaningful, decadal 5% to 95% (light blue) error ranges about that line are also given.

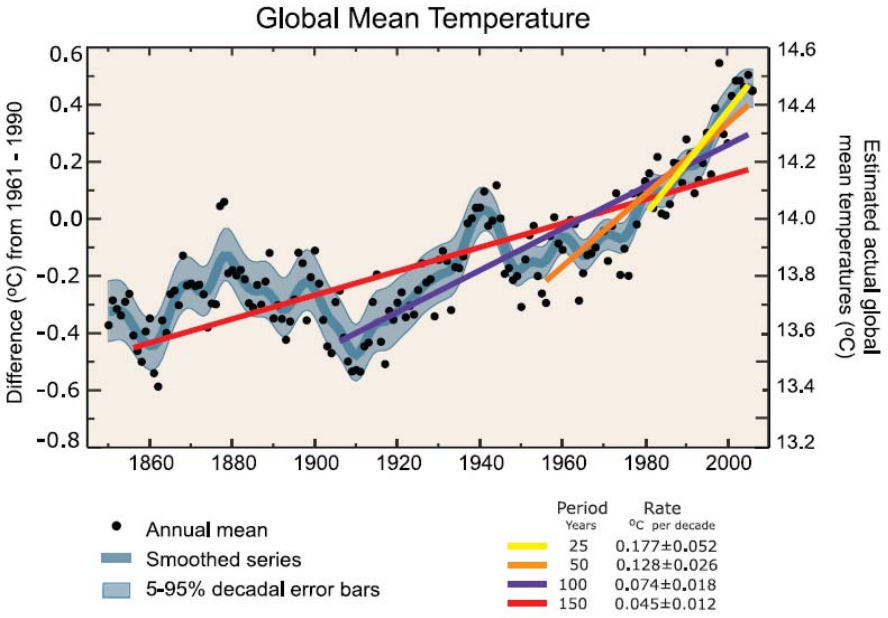

Figure 1.2: Variations of the Earth's surface temperature over the last 150 years [1.1]

In short, atmospheric CO_2 concentration, which is the most important anthropogenic greenhouse gas, rose from 280 to nearly 380 parts per million by volume (ppmv) over the last 150 years, almost entirely for anthropogenic causes, and in the same period of time, although the warming has been neither steady nor the same in different seasons or in different locations, the global average surface temperature has increased by about 0.7°C [1.1].

Important aspects of climate are quickly changing as a direct consequence of this global warming, and they have an incalculable impact on human life: agriculture, availability of fresh water, sea level, changes on the type, frequency and intensity of catastrophic events, like heat waves or floods, etc.:

- Precipitations have increased in eastern North and South America, northern Europe and northern and central Asia, but they have decreased in southern Africa, the Mediterranean and southern Asia. Widespread increases in heavy precipitation events have been observed, even in places where total amounts have decreased. These changes are associated with increased water vapor in the atmosphere arising from the warming of the oceans [1.1].

- The extent of regions affected by droughts has increased as precipitation over land has marginally decreased while evaporation has increased due to warmer conditions. Generally, numbers of heavy daily precipitation events that lead to flooding have increased. The frequency of tropical storms and hurricanes vary considerably from year to year, but all evidence points to a substantial average increase in intensity and duration since the 1970s [1.1].

- The amount of ice and snow on the Earth is decreasing, especially since 1980. Most mountain glaciers are getting smaller. Snow cover is retreating earlier in the spring. Sea ice in the Arctic is shrinking in all seasons. Reductions are reported in permafrost, seasonally frozen ground and river and lake ice. Important coastal regions of the ice sheets on Greenland and West Antarctica, and the glaciers of the Antarctic Peninsula, are thinning and contributing to sea level rise [1.1]

- There is strong evidence that global sea level gradually rose in the 20th century and is currently rising at an increased rate, after a period of little change between AD 0 and AD 1900. The two major causes of global sea level rise are thermal expansion of the oceans and the loss of land-based ice due to increased melting [1.1].

1.2 Alternative to Fossil Fuels

The magnitude of the problem led the International Community to the Kyoto Protocol agreement. The objective of the protocol is the "stabilization of greenhouse gas concentrations in the atmosphere at a level that would prevent dangerous anthropogenic interference with the climate system" [1.2] by assigning mandatory emission limitations to the signatory nations. In particular, the regulation affects emissions of six greenhouse gases: carbon dioxide, methane, nitrous oxide, sulfur hexaflouride, HFCs and PCFs.

In fact, these emission limitations suppose for the industrialized countries "a reduction between 1990 and 2010 of their collective emissions of greenhouse gases by 5.2%" [1.3]. Therefore, the need for industrial

nations to develop an energy policy designed to reduce carbon dioxide emissions is becoming widely recognized.
Let us review the energy conversion technologies that -if implemented on a large scale- would allow for a reduction on carbon dioxide emissions.
Technologies which are immediately available and economically viable:

0- Better building insulation.
1- Small-scale solar heating, particularly for domestic hot water.
2- Smaller cars and widespread use of the hybrid car
3- Combined heat and power plants (CHP), for industrial use, hospitals, building complexes, supermarkets, public buildings.
4- Wind farms, primarily on-shore
5- Bio-mass and waste-to-energy fuels.

Additional technologies that would become available within a 20 years span and that do not demand significant technological advance but need major capital investments [1.4]:

- Generation III nuclear reactors based on current commercial technology, but with an innovative design that increases plant safety, improves plant availability, and reduces plant capital and operating costs [1.5].
- Integrated gasification combined cycle power plants (IGCC), coupled with carbon sequestration and storage in appropriate strata.
- Offshore wind generation.

Advanced technologies that would require substantial research and development [1.4]:

- Hydrogen-fuelled transportation. Here the hydrogen fuel cell itself could perhaps be placed within our second category above, but for widespread application comprehensive hydrogen gas network must be developed and the source of the hydrogen also presents a problem. The safety implications of a hydrogen economy have also yet to be fully considered and costed.
- Generation III+ and Generation IV reactors, which would be relatively economical and proliferation resistant, with enhanced safety and minimized waste production. The latter are being designed to generate hydrogen from water decomposed by nuclear heat at high temperature [1.5].
- Photo-voltaic cells on a large scale.
- Fusion reactors.

1.3 Research Goals.

One of the proposed alternatives to fossil fuels is a future energy scenario based on renewable sources that uses hydrogen as a vector. However, as we have said before, its technical and economic viability still needs to be fully investigated.
The unavoidable short term strategy is still based on energy conversion from fossil fuels. In particular, highly efficient technologies are being developed to produce hydrogen from fossil fuels and to separate and store carbon dioxide.
This background information helps define the technological niche to which our project belongs as an Advanced Conversion System Analysis whose objective is to study the syngas desulfurization process, so that we can model and simulate it. This project is included in a larger research project: the study, analysis and simulation of a hydrogen-fed steam power plant based on the ZECOTECH© cycle in which the fuel is produced by coal gasification and CO_2 capture processes. The study is in progress at the Department of Mechanical and Aeronautical of the University of Roma 1, “La Sapienza”, within the frame of a National Research Project coordinated by the Italian National Agency for New Technologies, Energy and Environment (ENEA).
The goal of the broader national project is to develop to a pilot-plant stage a clean coal technology that can be used to produce hydrogen and electricity in this interim period until technologies based on renewable sources are fully investigated and developed.

SECTION 2 - DESCRIPTION OF THE PLANT

This section briefly describes the processes and devices that compose the plant for which our desulfurization system is being designed. Special attention is given to the coal gasification and carbon dioxide (CO_2) capture processes (called throughout this Report "chemical plant"), the configuration of the ZECOTECH© cycle from a thermodynamic point of view, and how they have been combined to optimize the overall process. Some comments on how the gas cleaning can be integrated in the whole plant arrangement are also offered.

2.1 Introduction

The study of the operational viability of the ZECOTECH© cycle (Zero Emission Combustion Technology) is part of the ZECOMIX project (Zero Emission Coal Mixed). This is a large research coordinated by ENEA, which has as objective the research and development of advanced systems for the generation of energy from solid fossil fuel sources with CO_2 sequestration.

In particular, the Department of Mechanical an Aeronautical Engineering of the University of Roma 1, "La Sapienza", is collaborating in the process configuration analysis.

In very general terms, the power plant is composed by two sections ("units"):

- A chemical unit that performs the gasification process and the CO_2 capture.
- A mechanical unit for electrical power production from the syngas produced in the chemical unit.

The gas cleaning to remove the particulates and the contaminants is intended to be implemented as an intermediate step in the chemical plant. This will be extensively discussed in Section 2.4.

2.2 Chemical Unit

The only technology for carbon dioxide sequestration developed to industrial level is the mono ethanol amine (MEA) removal. A likely alternative is the use of limestone (CaO) as CO_2 absorber. This technology is adopted today only in some pilot-scale plants [2.1]. A comparison between both options has been performed in detail in [2.2]. It should be noted that in both cases we generate a $H_2 + H_2O$ stream, which is then used as fuel in the mechanical unit, and a CO_2 stream.

To be a real "zero CO_2 emission" power plant, a carbon dioxide storage process should be included. We will return to this issue in Section 2.6.

A. CO_2 Separation Process Based on CaO

With this choice we need three reactors: the gasifier, the decarbonator and the decalcinator. As mentioned above, all process calculations (mass flow rates, pressure and temperatures) are reported in detail in [2.2]. Figure 2.2 represents the overall chemical plant.

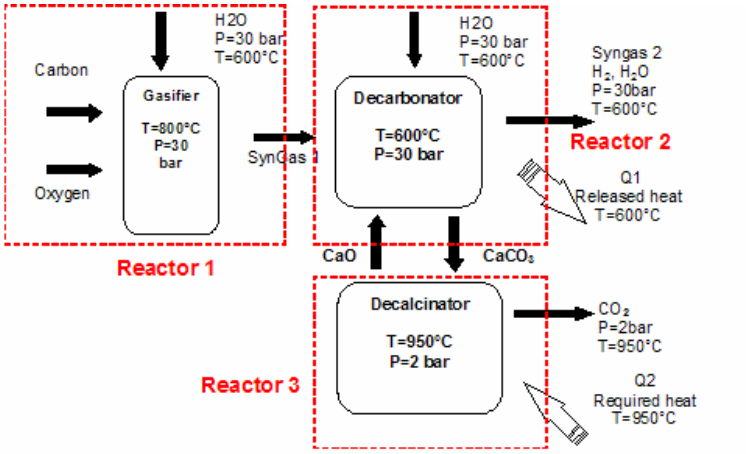

Figure 2.2: Coal gasification and CO_2 separation processes based on CaO [2.2]

The Gasifier
With reference to figure 2.2, coal gasification takes places in reactor 1. The input rates are designed to make the process thermally neutral, and maintain the reactor at 800ºC.
The partial oxidation reaction for carbon is:

$$C + \tfrac{1}{2} O_2 \rightarrow CO$$

This reaction is exothermic and thus water is introduced into the gasifier, in this case in the form of steam, to moderate the temperature by the endothermic reaction:

$$C + H_2O \rightarrow H_2 + CO$$

Other reactions that occur within a gasifier are the shift reaction:

$$CO + H_2O \rightarrow H_2 + CO_2$$

And the hydrogasification reaction:

$$C + 2H_2 \rightarrow CH_4$$

The gases leaving the gasifier are essentially free of hydrocarbons heavier than methane (CH_4), the sulfur present in the feed has evolved mostly to hydrogen sulfide (H_2S) with some residual carbon-oxide sulfide (COS), and the nitrogen to compounds such as ammonia (NH_3) and hydrogen cyanide (HCN) [2.5]

The Decarbonator

In reactor 2, the CO and CH_4 coming from the gasifier react with H_2O into CO_2 and H_2:

$$CO + H_2O \rightarrow H_2 + CO_2 \qquad \text{(shift reaction)}$$

$$CH_4 + H_2O \rightarrow 4H_2 + CO_2$$

Furthermore, the CO_2 is absorbed by the CaO, generating calcium carbonate ($CaCO_3$) as by product:

$$CaO + CO_2 \rightarrow CaCO_3$$

The overall process is exothermic, and a significant quantity of heat is released [2.2]

The Calcinator
In this reactor the CaO is regenerated, and the CO_2 is finally released:

$$CaCO_3 \rightarrow CaO + CO_2$$

This reaction is endothermic, so an external heat input is necessary. For process optimization reasons, the reaction takes place here at 2 bar and 950ºC [2.2]

B. CO_2 Separation Process Based on MEA
In this case we have two main sections: section 1 that includes the gasifier and the shift reactor, and section 2 that represents the CO_2 removal process.
Again, for a thorough explanation the reader is referred to reference [2.2]. Here, we shall only give a general functional description of the process.
Figure 2.3 represents the overall chemical plant.

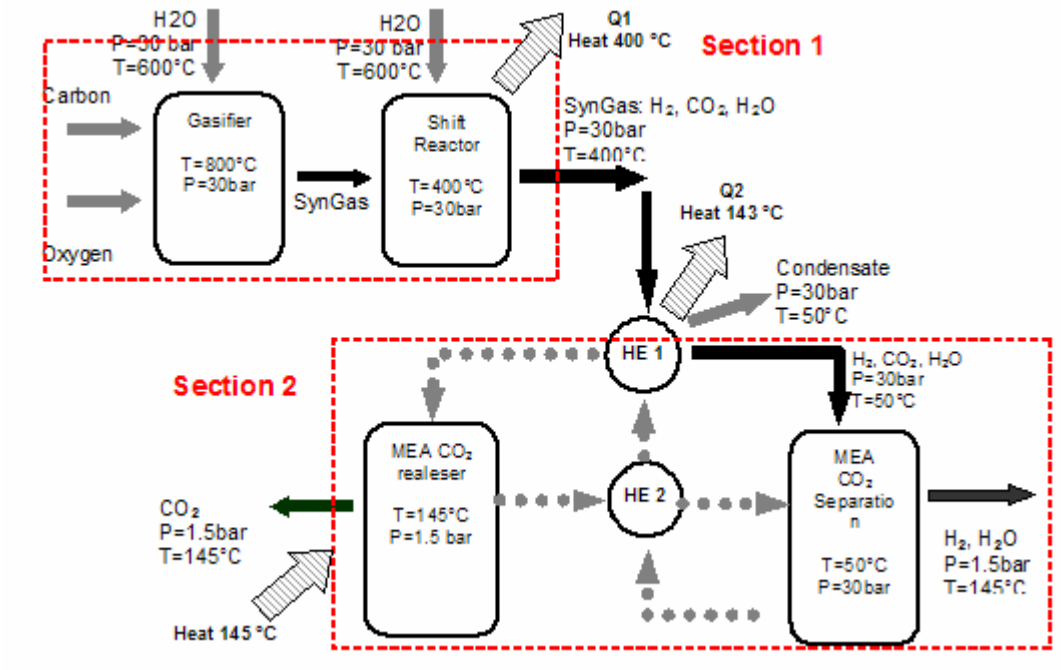

Figure 2.3: Coal gasification and CO_2 separation processes based on MEA [2.2]

Unit 1

The reactions are identical to the ones described previously in the gasifier and decarbonator section, except that $CaCO_3$ is not been generated because there is not CaO in the system. Again, the overall process is exothermic, and a considerable amount of heat is released [2.2]

Unit 2

A MEA solution is used to absorb the CO_2 present in the syngas. This process occurs at high pressure and low temperature. In the recycle phase, the MEA/CO_2 solution is heated and depressurized, and CO_2 is released.

2.3 Mechanical Unit: the ZECOTECH© Cycle

The mechanical portion of the plant is based on the ZECOTECH© Cycle, an innovative combined cycle in which steam is used in both the topping and the bottoming sections. The hydrogen is used to produce high temperature, medium pressure steam that evolves in the turbine in the topping cycle following approximately a Brayton cycle: the exhaust steam is used in a heat recovery boiler to produce steam at medium-temperature, high-pressure that powers a traditional steam power cycle.

This configuration can reach a 65% (first law) efficiency, and if the combustion chamber is replaced by a more intensive reburning, even 70% is feasible [2.2]. Figure 2.3 shows the thermodynamic cycle on the Mollier's diagram:

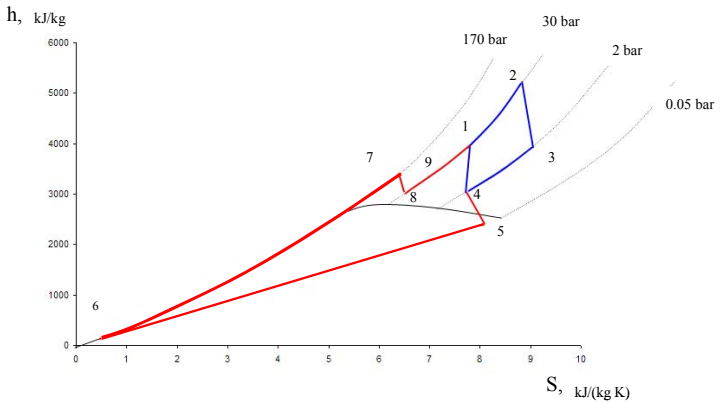

Figure 2.3: The ZECOTECH© cycle drawn on the Mollier's diagram [2.6]

- Combustion process (1-2): hydrogen coming from the chemical unit enters the combustion chamber (a) at a pressure of 30 bar. Recovered and compressed steam is also introduced as an attemperator. High temperature and medium pressure steam, 30 bar and 1000ºC, is produced by burning the H_2.

- High temperature expansion (2-3): steam expands in the high temperature turbine (d) down to 2 bar and about 600ºC.

- Heat recovery (3-4): the steam is cooled down from state 3 to 245ºC in a heat recovery boiler (g) producing secondary steam at 170 bar and 600ºC for the bottoming process 6-7.

- Low pressure expansion (4-5): part of the low pressure steam generated in the heat recovery boiler (g) expands in a conventional low pressure turbine (c) down to 0.05 bar and 35ºC.

- Compression (4-1): the rest of the low pressure steam from the recovery boiler is compressed (f) to 30 bar.

- Water condensation (5-6): water is cooled with a standard condenser (e) at 0.05 bar. Part of this cooled water is directed to the heat recovery boiler (g) producing secondary steam for the bottom cycle (process 6-7), and the remaining is discharged.

- High pressure expansion (7-8): the secondary steam produced by the heat recovery boiler (g) expands in a conventional turbine down to 30 bar and 350ºC.

- Steam flow mixer (8-1): the steam flows coming from the compressor (f) and the high pressure turbine (d) are mixed and sent to the combustion chamber (a). The number 9 in the Mollier's diagram of figure 2.3 points to the steam state after the mixing process. Figure 2.4 shows a block diagram of the processes just illustrated.

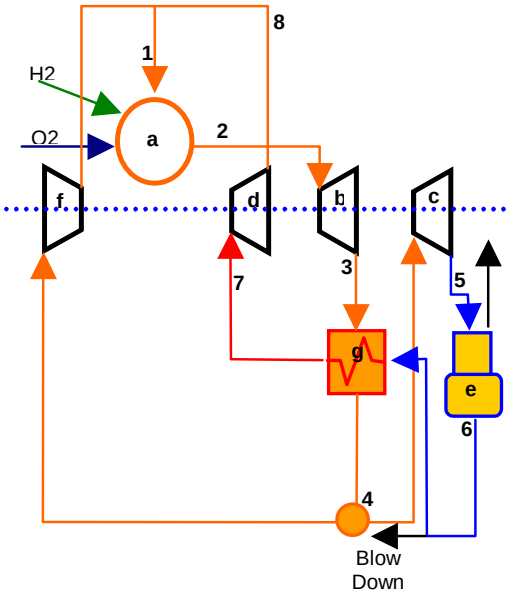

Figure 2.4: The ZECOTHEC© process configuration. The numbering refers to the cycle representation on the Mollier's diagrams of figure 2.2 [2.2]

2.4 Optimal Configuration

A comparison of both chemical plants (MEA and CaO) coupled with the same mechanical plant has been performed in [2.2]. Since both CO_2 separation processes require heat supply, several alternative configurations have been proposed in order to better exploit the "waste heat flows" within the power plant, with the objective of maximizing the overall plant efficiency.

The conclusion of this comparison is that the CaO removal technology is better suited to be coupled with a mechanical plant based on the ZECOTECH© Cycle, because it has a higher performance (42.5% overall plant efficiency), and it is also more economically profitable [2.2]. Figure 2.5 shows the plant configuration proposed as "optimal".

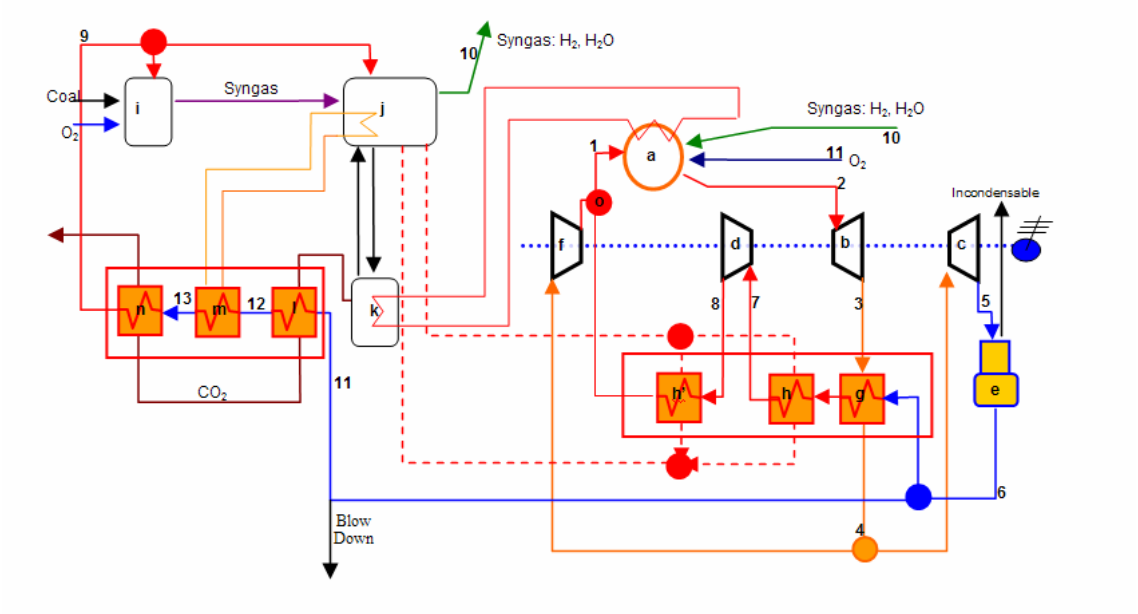

Figure 2.5: Proposed configuration [2.2]

The main modifications enacted are:

- The combustion chamber (a) is cooled in order to supply the calcinator (k) reactor energy.
- Two heat exchangers (h & h') recover some heat from the decarbonator (j) to integrate the recovery boiler (g) and to preheat the steam that goes into the combustion chamber (a).
- A heat exchanger (m) uses part of the heat released by the decarbonator (j) to generate the steam required by the gasifier (i).

2.5 Syngas Cleaning System Integration

During gasification of a carbonaceous material, fuel-bound impurities that are naturally present will convert into gaseous contaminants, such as: H_2S, COS, NH_3, HCN, HCl, and alkali (sodium, potassium, etc.) macromolecules [2.7]. These species must be removed to sub-ppm levels to meet pollutant emission limits in power generation applications, or contaminant tolerance limits for fuel cell and chemical production applications (normally, the latter are much more stringent [2.7]).

This crucial gas cleaning step was not included in the original power plant model on which the optimization study has been based: that simulation simply considered that the gaseous contaminants were separated from the rest of the syngas (with no energy consumption) as they were transported from the gasifier to the decarbonator.

One of the main objectives of this project is to remedy this neglection by modeling a part of the syngas cleaning system: the sulfur removal process. To this purpose, several technologies will be considered, and the selected option will be inserted in the chemical plant between the gasifier and the decarbonator: the gases produced in the gasification process will first go through the desulfurization device where the sulfur compounds will be removed, and then to the decarbonator reactor to continue with its treatment.

2.6 Carbon Dioxide Capture and Storage

A power plant will be "zero CO_2 emission" only if a carbon dioxide storage procedure is included: this step usually includes a compression and transport for storage in geological formations (such as oil and gas fields, unminable coal beds and deep saline formations), in the ocean (direct release onto the deep seafloor), or for use in industrial processes (fixation of CO_2 onto inorganic carbonates). Only the first two options have been comprehensively studied [2.3].

Storage of CO_2 in deep, onshore or offshore geological formations uses many of the same technologies developed by the oil and gas industry. In particular, carbon dioxide injection in oil fields is a proven technique that is being currently used to enhance oil recovery. An overview of geological storage options is provided in figure 2.1.

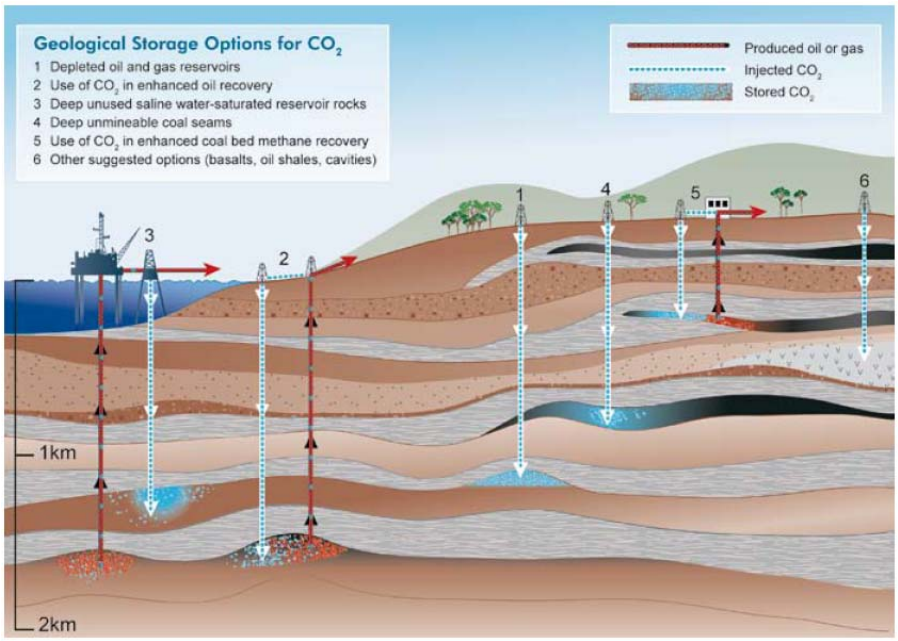

Figure 2.1: Geological storage options [2.4]

Apart for the readiness of this technology, it has an enormous potential for stabilizing atmospheric greenhouse gas concentration: there is a technical storage capacity of at least 2000 $GtCO_2$, which is 150 times bigger than annual worldwide large stationary CO_2 source emissions [2.4]. Moreover, the local health, safety and environment risks of geological storage are apparently very small, comparable in any case to the risks of current activities such as natural gas storage [2.4]. These three points: technological readiness, massive CO_2 storage potential, and safety, make the dioxide carbon capture and storage (CCS) a very attractive option to reduce the greenhouse emissions in the short term. Furthermore, it is worth mentioning that application of CCS to electricity production is estimated to increase electricity generation costs only by about 0.01–0.05 $/kWh (2002 conditions) [2.4]. Since though the analysis of the CCS alternatives is not within the scope of this study, we will only assume here that a sufficient number of fully operative CO_2 storage facilities are available.

SECTION 3 - SULFUR OXIDES

This section enumerates the contaminants that can be produced during coal gasification process and describes their effects on the environment. Since the objective of this project is to study the removal of hydrogen sulfide, we pay special attention to this pollutant, which is a precursor for sulfur dioxide that has to be eliminated in order to make syngas suitable for use in power generation due to evermore stringent emission standards. Next we analyze desulfurization technologies, providing an overview of their operation. Finally we discuss the ones that are more appropriate for syngas cleaning.

3.1 Introduction: Air Pollutants

During gasification of carbonaceous materials, fuel-bound constituents convert to different gaseous compounds, such as: hydrogen (H_2), methane (CH_4), carbon dioxide (CO_2), carbon monoxide (CO), hydrogen cyanide (HCN), hydrogen sulfide (H_2S), hydrogen chloride (HCl), ammonia (NH_3), water (H_2O), and chlorine (Cl_2). Others appear as solid phases, for instance: silicon dioxide (SiO_2), calcium carbonate ($CaCO_3$), calcium oxide (CaO), unburned carbon (C), crystalline sulfur (S), and alkali macromolecules.

Some of them must be removed before the syngas can be used for H_2 production. In addition, others are also contaminants whose emissions into the atmosphere are regulated by law. These are:

- **Particulate Matter (PM)**. They are solid particles and liquid droplets found in the gaseous stream. Some of them, known as primary particles, are emitted directly from a source. Others, known as secondary particles, form after complicated reactions in the atmosphere of chemicals such as sulfur dioxides and nitrogen oxides. The biggest anthropic source of particles is combustion.

The size of particles is directly linked to their potential for causing health problems. Inhalable coarse particles, with diameters larger than 2.5 micrometers and smaller than 10 micrometers, can find their way deep into the lungs and cause serious health problems [3.1].

Emissions of particle matter into the air from large combustion plants are regulated in the European Union [3.2]

	O_2 content	50 – 100 MWt	> 100 MWt
Solid fuels	6%	50	30
Liquid fuels	3%	50	30
Gaseous fuels	3%	5	5

Table 3.1: Emission limits for particle matter by new plants [mg/Nm^3] [3.2]

- **Hydrogen sulfide (H_2S)**. It forms sulfur dioxide (SO_2) when combusted.

$$2H_2S + 3O_2 \rightarrow 2H_2O + 2SO_2 \quad (Eq.\ 3.1)$$

The sulfur dioxide belongs to the family of sulfur oxide gases (SO_x), which cause a wide variety of health and environmental impacts [3.1]. They:

- aggravate respiratory illness.
- react with other substances in the air to form acid rain, which damages trees and crops, and makes soils, lakes, and streams acidic.
- contribute to the formation of atmospheric particles.

Emissions of sulfur dioxide into the air from large combustion plants are regulated in the European Union [3.2]

	O_2 content	50 – 100 MWt	100 – 300 MWt	> 300 MWt
Solid fuels	6%	850	200	200
Biomass	6%	200	200	200
Liquid fuels	3%	850	400 - 200	200
Gaseous fuels	3%	35	35	35
Liquefied gas	3%	5	5	5

Table 3.2: Emission limits for SO_2 by new plants [mg/Nm^3] [3.2]

- **Carbonyl sulfide (COS)**. Limited information is available on the health effects of carbonyl sulfide. Acute (short-term) inhalation of high concentrations of carbonyl sulfide may cause narcotic effects in humans. It may also irritate the eyes and skin [3.4].

- **Hydrogen chloride (HCl)**. Catalysts such as Cu and Zn used for shift reaction (conversion of CO in the syngas to H_2) and zinc titanate sorbents, which used in high temperature desulfurization, are poisoned by HCl vapor in the feedstock. Furthermore, chlorine species can induce corrosion of the turbine blades. In addition, allowable HCl concentration in the feed gas to a fuel cell is prescribed to be less than 0.5 ppmv [3.3], because halogen compounds lead to severe corrosion of cathode hardware.

- **Ammonia (NH_3) and hydrogen cyanide (HCN)**. They are readily converted to oxides of nitrogen (NO_x) during the combustion of syngas.

The chief causes of concern with NO_x are:

- ground-level ozone (smog) is formed when NO_x and volatile organic compounds (VOCs) react in the presence of sunlight, which can trigger serious respiratory problems.
- it reacts to form nitrate particles, which cause respiratory problems.
- NO_x and sulfur dioxide react with other substances in the air to form acid rain.
- increased nitrogen loading in water bodies, contributes to nutrient overload that deteriorates water quality.
- in the air, NO_x reacts readily with common organic chemicals and even ozone, to form a wide variety of toxic products, for example: the nitrate radical, nitroarenes, and nitrosamines.
- one member of the NO_x, nitrous oxide (N_2O), is a greenhouse gas, and it accumulates in the atmosphere.

Emissions of oxides of nitrogen into the air from large combustion plants are regulated in the European Union [3.2]

	O_2 content	50 – 100 MWt	100 – 300 MWt	> 300 MWt
Solid fuels	6%	400	200	200
Biomass	6%	400	300	200
Liquid fuels	3%	400	200	200
Natural gas	3%	150	150	100
Other gases	3%	200	200	200
	single gas turbine unit			
Liquid fuels	15%	120	120	120
Natural gas	15%	50	50	50
Other gases	15%	120	120	120

Table 3.3: Emission limits for NO_x (measured as NO_2) by new plants [mg/Nm^3] [3.2]

- **alkali (sodium/potassium macromolecules)**. These alkali species are known precursors of corrosion-inducing condensates formed on gas turbine blades.

3.2 Desulfurization Technology

There exist numerous methods to remove sulfur pollutants gases. Some are based on well proven technologies, for example wet scrubbers, and are widely adopted in present fossil-fuelled plants. Whereas others still are being objects of research, for instance the membrane separation technology, or are in the pilot plant demonstration stage, such as the hot gas desulfurization.

A. Scrubbing Processes

The sulfur dioxide (SO_2) scrubbing processes include wet scrubbing, dry sorbent injection and spray dryer absorption. They use an alkaline reagent which is injected in the flue gas in a spray tower or directly into the duct. The SO_2 is absorbed by the alkaline reagent and neutralized into a solid compound, which is then removed from the waste gas stream downstream.

1. Wet Scrubber Systems

They achieve high removal efficiencies, typically greater than 90%, and have a large operational range: they have been applied to combustion units from 5 MW to over 1,500 MW. Typical inlet gas temperatures are from 150°C to 370°C [3.5].

Many different types of absorbers have been used in wet systems, including, venturis, plate towers, and mobile packed beds, but the present trend is to use simple scrubbers such as spray towers, because the formers present problems of plugging, erosion and scaling [3.6].

An archetypal wet scrubber system is shown in figure 3.1: flue gas is ducted to a spray tower where an aqueous slurry stream of sorbent is injected into the flue gas. To provide good contact between the waste gas and sorbent, the nozzles and injection locations are designed to optimize the size and density of slurry droplets formed by the system. The waste gas stream becomes saturated with water evaporated from the slurry, which facilitates sulfur dioxide dissolution into the slurry droplets, where it reacts with the alkaline particulates forming a neutral salt. The slurry falls to the bottom of the absorber where it is collected. Treated flue gas passes through a mist eliminator before exiting the absorber which removes any entrained slurry droplets. The treated gas is though still saturated with water and contains some SO_2, which makes it highly corrosive to any downstream equipment, so it is usually reheated above its dew point.

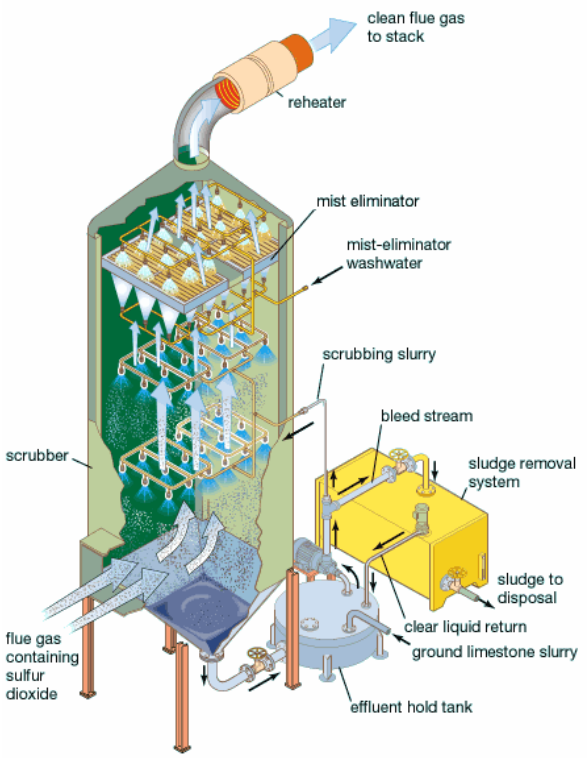

Figure 3.1: Flue gas desulfurization limestone wet scrubber [3.7]

Typical sorbent materials are limestone ($CaCO_3$) and lime ($Ca(OH)_2$), both of them producing calcium sulfite ($CaSO_3$):

$$CaCO_3(s) + SO_2(g) \rightarrow CaSO_3(s) + CO_2(g) \quad \textit{(Eq. 3.2)}$$

$$Ca(OH)_2(s) + SO_2(g) \rightarrow CaSO_3(s) + H_2O(l) \quad \textit{(Eq. 3.3)}$$

Some flue gas desulfurization systems go one step further and oxidize the calcium sulfite ($CaSO_3$) to produce gypsum ($CaSO_4 \cdot 2H_2O$), which is a useful and marketable by-product [3.8]:

$$CaSO_3(s) + \tfrac{1}{2}O_2(g) + 2H_2O(l) \rightarrow CaSO_4 \cdot 2H_2O(s) \quad \textit{(Eq. 3.4)}$$

Sodium-based solutions provide better SO_2 solubility and less scaling problems than lime or limestone. However, sodium reagents are much more expensive [3.6].

Wet limestone scrubbing has high capital and operating cost due to the handling of liquid reagent and waste. Nonetheless, it is the preferred process for electric utility power plants burning coal due its high efficiency and to the low cost of limestone [3.5].

Unit size [MW]	Capital cost [$/kW]	O&M cost [$/kW]	Annual cost [$/kW]	Cost per mass of pollutant removed ($/ton)
> 400	100 - 250	2 - 8	20 - 50	200 – 500
< 400	250 - 1,500	8 - 20	50 - 200	500 – 5,000

Table 3.4: Summary of cost information for wet scrubbers (2001 dollars) [3.5]

2. Dry Sorbent Injection Systems

These devices are less efficient than wet scrubbers, typically less than 80%, and are only applied to small combustion units, generally smaller than 300 MW. Optimal temperatures for SO_2 removal vary between 150°C to 1000°C depending on the sorbent properties [3.5].

In a dry sorbent injection system, as the one shown in figure 3.3, powdered sorbent is directly injected into the furnace, the economizer, or the downstream boiler ducts. Then the dry waste product is removed using particulate control equipment, like electrostatic precipitators or fabric filters.

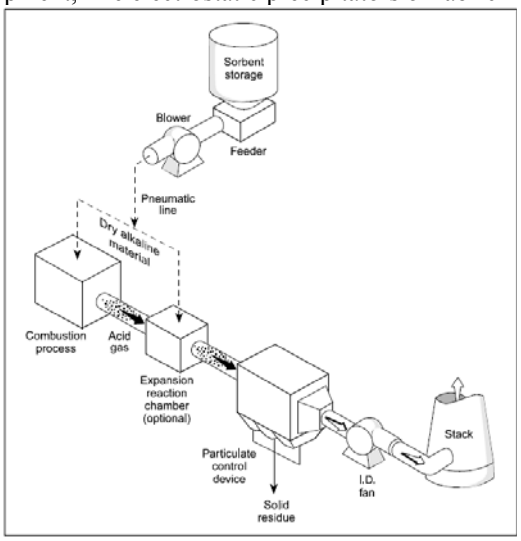

Figure 3.2: Components of dry injection system [3.9]

An even distribution of sorbent and adequate residence time at the proper temperature is critical for high SO_2 removal rates. Usually, these systems use calcium hydroxide and sodium based alkaline reagents that have the consistency of fine powder. These fine particles have large surface areas that facilitate the adsorption process [3.9].

Dry scrubbers removal efficiency is significantly lower than that of wet systems. However, also significantly lower are the capital and annual costs, which, together with their ease of installation, smaller size and simpler waste disposal system, makes them good candidates for retrofit

3. Spray Dryer Systems

They are also called semi-dry scrubbers. Their efficiency lies between that of the wet scrubbers and that of the dry sorbent injectors. They are only applied to small combustion units, generally smaller than 300 MW, as the dry sorbent injectors. Optimal temperatures for SO_2 removal range from 150°C to 180°C [3.5].

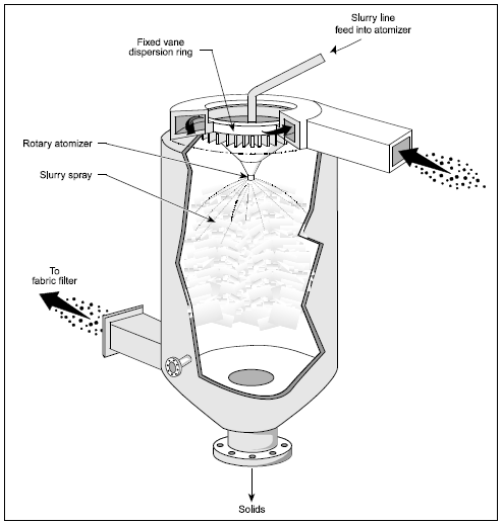

Figure 3.3: Spray dryer absorber [3.9]

A spray dryer system combines concepts of the two previous ones. A schematic representation is shown in figure 3.3. As in the wet scrubbing process, an aqueous slurry stream of sorbent is injected into the flue gas. However, in this case the slurry has a higher sorbent concentration, and the absorption chamber is designed to provide sufficient contact and residence time to produce a dry product at its exit.
Various calcium and sodium based reagents can be utilized as sorbent, lime being though the typical reagent since it is more reactive than limestone and less expensive than sodium based compounds. The reagent slurry is injected through rotary atomizers or dual-fluid nozzles to create a fine droplet spray, that are also much more complicated and expensive to operate that the injection equipment required by dry sorbent injection [3.9].
The capital and operating cost for spray dry scrubbers are lower than for wet scrubbing because no equipment is needed to handle wet waste products. Typical applications include electric utility units burning low-content sulfur coal, and industrial and municipal waste incinerators [3.5].

Unit size [MW]	Capital cost [$/kW]	O&M cost [$/kW]	Annual cost [$/kW]	Cost per mass of pollutant removed ($/ton)
> 200	40 - 150	4 – 10	20 - 50	150 – 300
< 200	150 - 1,500	10 - 300	50 - 500	500 – 4,000

Table 3.5: Summary of cost information for semi-dry scrubbers (2001 dollars) [3.5]

B. Fluidized Bed Combustion Systems
Fluidized bed combustion (FBC) is a technology that suspends solid fuels within a rising column of air during the combustion process, which results in a turbulent mix of gas and solids. The turbulent mixing increases the rate and efficiency of the combustion process and it allows to burn high moisture content or low heating value fuels (like lignite and sub-bituminous coal, agricultural waste, municipal solid waste, wood wastes, etc.) that are difficult to process with other technologies [3.10].
The same turbulent mixing of the coal that improves combustion also provides a way to inject sulfur-absorbing chemical, such as limestone ($CaCO_3$) or dolomite ($CaMg(CO_3)_2$), to precipitate sulfate while the combustion process proceeds. More than 95% of the sulfur pollutants in coal can be captured inside the boiler by the sorbent, which eleminates the need of external sulfur emission controls, such as scrubbers [3.11].
Furthermore, since FBC allows coal to burn at lower temperatures, less NO_x is also emitted [3.12].

C. Membranes
Membrane separation is a relatively new technology wherein polymer membrane modules separate gases by selective permeation of one or more gaseous components from one side of a membrane barrier to the other side. The membrane selectivity is based on the solubility of the gas compounds in the polymer. Generally, larger, more condensable molecules are more soluble in polymers than smaller, permanent ones. So, polymeric membrane materials have been developed that selectively permeate acid or polar gases, such as H_2S and CO_2, in mixtures with light gases, such as H_2 and CO. Gas components are transported across the membrane as a result of a concentration gradient.

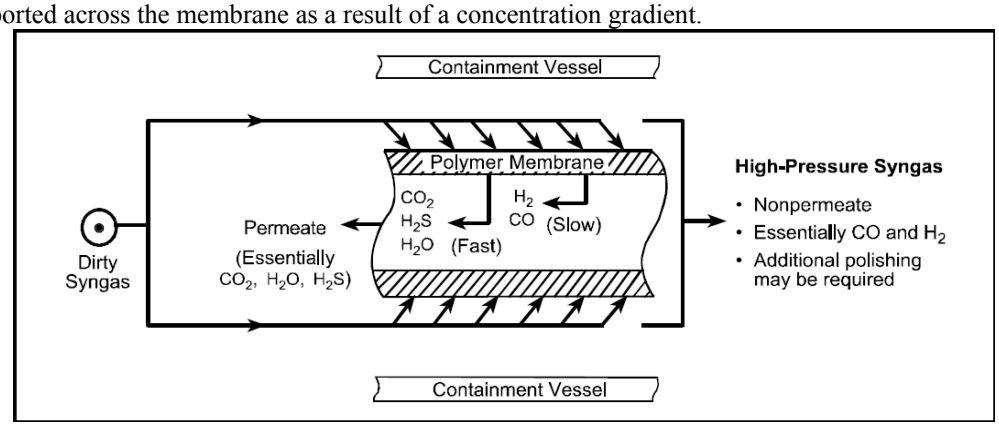

Figure 3.4: Separation of acid gases from syngas in polymer membrane module [3.13]

Commercial polymer membrane modules are renowned for their simplicity, reliability, and effectiveness of operation. The disadvantage of membranes is that regardless of the selectivity of a polymer membrane for acid gas components, there is always a finite permeability for hydrogen and carbon monoxide that

implies some of these gases are removed with the pollutants. The fact that acid gases are present at trace concentrations also means the driving force for permeation of the acid components is much smaller than for primary syngas components like H_2 and CO. This factor becomes more pronounced as the contaminant concentration in the syngas drops as a consequence of contaminant removal. Thus, preliminary membrane simulation studies suggest that only a 60 to 90% removal of the H_2S would be practical [3.13]. Additional H_2S removal would require an extra polishing sulfur removal step, such as a regenerable ZnO coated monolith. This possibility, named hybrid sulfur removal process, is actually being investigated, but first the membrane operating conditions should be expanded above the current limit (100ºC) [3.13].

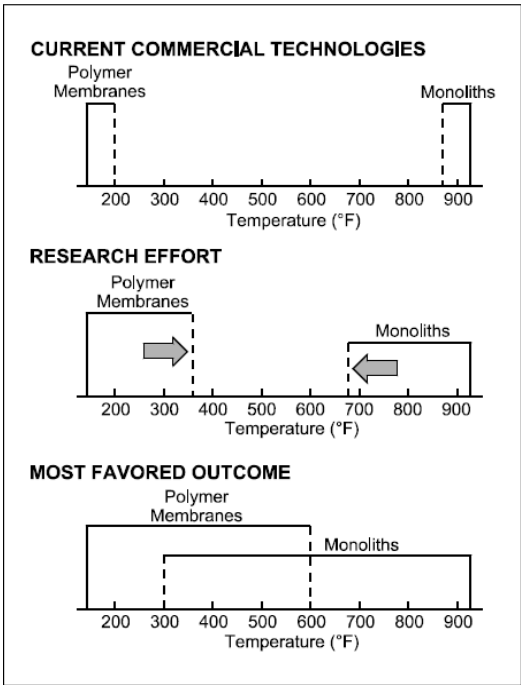

Figure 3.5: Hybrid process for syngas desulfurization [3.13]

D. Hot Gas Desulfurization

In conventional gasification cleanup systems, costly heat exchangers are necessary to cool down the fuel gases for cleaning, sometimes to temperatures as low as 100ºC, and to reheat the gases prior to injection into the turbine. The result is significant losses in efficiency for the overall power cycle, and is an infringement of the Second Law Design Guidelines. High-temperature coal gas cleanup system can be operated at conditions compatible with the gasifier and turbine components, resulting in a more efficient overall system [3.14]. Typically, hot gas desulfurization has been performed by using disposable zinc oxide. This method is very effective and sub-ppm H_2S concentrations in the effluent are easily reached, but the expense of continuously replacing this material unfavorably affects the cost of the treatment making it less attractive than other competing technologies.

Recently, hot gas desulfurization technologies based on regenerable sorbents have been developed to counteract this disadvantage: after the sorbent is sulfided, it is transported to another reactor where it undergoes oxidative regeneration, hence it can be used again to retain more syngas sulfur compounds.

Early work on this regenerable technology employed single oxide sorbents, especially iron oxide and zinc oxide. The sulfidation kinetics of the former are much quicker, but the latter ended up prevailing because of more favorable sulfidation thermodynamics, which makes it more attractive from the standpoint of H_2S removal efficiency.

However, the regenerability of ZnO is restricted by its tendency towards reduction to volatile elemental zinc. A well proved solution is to add TiO_2 into ZnO to stabilize it.

Thus, the actual trend in regenerable hot gas desulfurization (RHGD) is to use zinc titanate sorbents because they present the following advantages [3.15]:

- They exhibit lower rates of zinc loss than zinc oxide during sulfidation.
- Zinc titanates have intrinsic sulfidation kinetics comparable to those of zinc oxides.
- They have similarly high hydrogen sulfide removal efficiency as zinc oxides.
- Sulfided zinc titanate sorbents are fully regenerable.
- Zinc titanate sorbents can be sulfided completely.

Several laboratory experiments have demonstrated that zinc titanate sorbents are capable of reducing the COS and H_2S level in syngas to about 10 ppmv in both air blown and oxygen-blown syngas [3.14, 3.15, 3.16, 3.17, and 3.18].

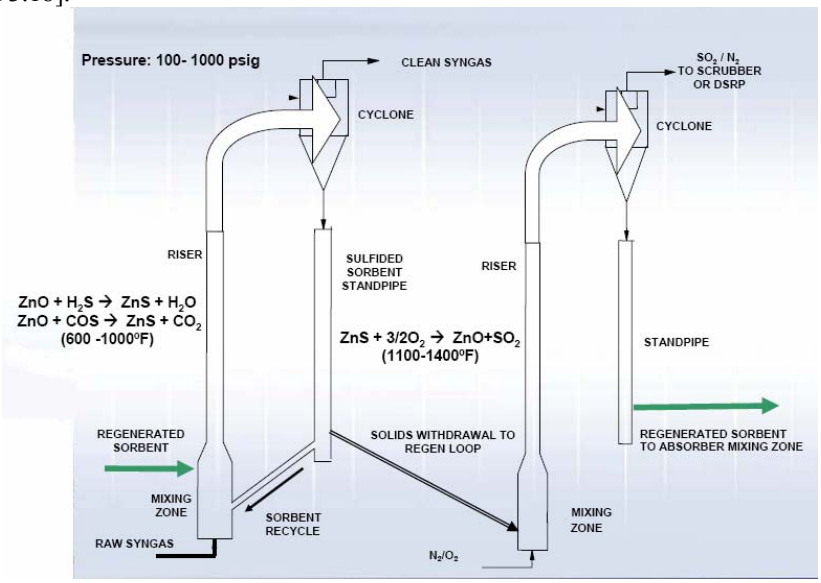

Figure 3.6: Hybrid process for syngas desulfurization [3.20]

At present, the major issue associated with RHGD is the need for the technology to be demonstrated for an extended period at a scale equivalent to commercial operation [3.19]. The most important effort aimed at testing this technology at industrial level is a pilot scale plant built by RTI International and Eastman Chemical Company in 2005, of which a schematic representation is shown in figure 3.6.
The experimental results from 2005 to date are very promising [3.20]:

- Sorbent can reduce total sulfur to 0.5 - 5 ppmv (> 99.7% sulfur removal).
- Regenerated sorbent has similar ability to absorb sulfur.
- It is economically feasible with respect to competing technologies.

It is expected that this process will be commercially available in 2009.
Another aspect to consider is that the regeneration of the sulfided sorbent produces a SO_2 rich off-gas, at high temperature and high pressure, which must pass through a sulfur fixation process. The usual approach consists in feeding a sulfator where sulfides are oxidized to sulfates for disposal.
Alternatively, the patented Direct Sulfur Recovery Process (DSRP) being developed by the Research Triangle Institute (RTI) is a highly attractive option for recovery of sulfur from this regeneration off-gas. Using a slipstream of coal gas as a reducing agent, it efficiently converts -over a catalyst- the SO_2 to elemental sulfur, a commercial product that is easily stored and transported [3.19].
The single-stage process, integrated with a metal oxide sorbent regenerator, is shown in figure 3.7.

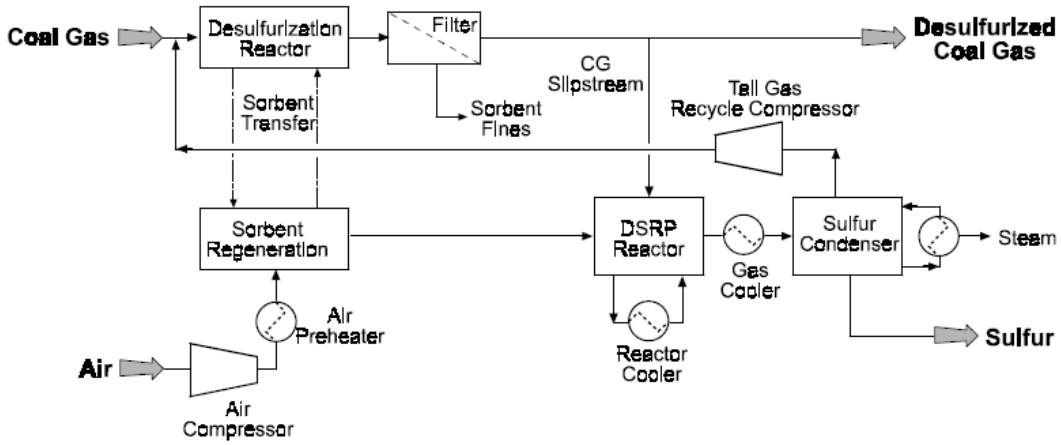

Figure 3.7: Hot gas desulfurization with DSRP [3.21]

Since the tail gas from the DSRP can be recycled as shown, there are no net sulfur emissions from the DSRP.

3.3 Conclusion: the selected alternative

Among the available alternatives to desulfurize syngases the most promising option is the hot gas desulfurization through a regenerable sorbent. As discussed at the beginning of this Section, traditional desulfurization technologies such as wet scrubbing require the syngas to be cooled before cleaning, so that it must then be reheated prior to its reinjection into the power cycle. This cooling-heating process is thermodynamically unacceptable and results also in a costly wastewater treatment. Hot gas desulfurization disposes of this problem because the syngas is treated at the high pressure and temperature conditions at which it leaves the gasifier:.

Results to date have demonstrated the technical ability to clean hot gases, and long term reliability tests, being presently developed [3.20], are attempting to establish the long term durability record required for commercial acceptance.

In summary, we think this is the best option to be studied in detail here because:

- By modeling the processes and devices needed for this regenerable hot gas desulfurization, we will achieve a more complete understanding of the scientific fundamentals underlying this new technology.

- The process fits perfectly with the philosophy of the plant in which it will be integrated: a hydrogen-fed steam power plant based on the ZECOTECH© cycle, where the fuel is produced by coal gasification and CO_2 capture processes. They are based on relatively new technologies, that have not been yet fully investigated or proved at a commercial scale level, but they show some promise of reaching a commercial stage in a relatively short period of time. Furthermore, all of the steps in the procedure take full advantage of the existing resources by maximizing the overall process efficiency.

- The optimization of this component as a part of a complete hydrogen-fed steam power plant will demonstrate the potential of this desulfurization technology, pinpointing its advantages and drawbacks with respect to other existing sulfur capture alternatives.

SECTION 4 - PHYSICAL MODELING

This section describes all the aspects of hot gas desulfurization systems and the model we will use to simulate it. We first introduce some assumptions to simplify the real physical and chemical desulfurization processes, so that it may be represented by a suitable set of equations. We next enumerate these equations, analyzing which variables are the unknowns, which ones are the boundary conditions, and which ones must be introduced as design parameters by the user. This study also compares different approaches to define the design parameters of the system.

4.1 Assumptions of the Model

The first element we will review is the sorbent. This is a key factor, since it is the responsible for capturing sulfur syngas compounds, that is, H_2S and COS, and, subsequently, releasing the sulfur as SO_2 when regenerated. Following sorbent composition selection, we will analyze the reactor design, which is the next most critical feature of a regenerable hot gas desulfurization process. A two-reactors system is necessary because of the cyclic nature of the process.

A. Regenerable Zinc Oxide – Titanium Dioxide Sorbents

As recalled in the previous section, sorbents made of ZnO and TiO_2 currently prevail, because they exhibit an excellent combination of properties: high hydrogen sulfide removal efficiency, elevated sulfur capacity, complete regenerability, good sulfidation kinetics and satisfactory stability.

Bulk mixed oxide solids of zinc and titanium are prepared by synthesizing highly dispersed mixed oxides from amorphous citrate precursors. In brief, this method consists in dehydrating, first rapidly (~15 min) in a rotary evaporator under vacuum and then slowly (3-24 h) in a vacuum oven at 70ºC, an aqueous solution of zinc acetate, titanium (IV) isopropoxide and citric acid to form a highly porous solid foam. The solid foam is then calcined in air in a muffle furnace at 550-850 ºC for 4-12 h, producing a porous, homogeneous mixed metal oxide (more details about preparation and characterization of sorbents in reference 4.1 and 4.2).

The most commonly found compounds in the ZnO-TiO_2 system are zinc oxide (ZnO), zinc orthotitanate (Zn_2TiO_4), zinc metatitanate ($ZnTiO_3$), $Zn_2Ti_3O_8$ and titanium dioxide (TiO_2). The types of phases present depend on the Zn/Ti atomic ratio and the calcination temperature [4.2]:

- The observed phase transformation with increasing temperature is $Zn_2Ti_3O_8 \rightarrow ZnTiO_3 \rightarrow Zn_2TiO_4$.
- Decreasing the Zn/Ti ratio of the solids produces phases in the order $ZnO \rightarrow Zn_2TiO_4 \rightarrow ZnTiO_3$ and $Zn_2Ti_3O_8 \rightarrow TiO_2$.

Several examples of zinc titanate sorbents are enumerated in table 4.1.

sorbent	(Zn/Ti) (atomic ratio)	crystalline phases (wt %)				
		ZnO	Zn_2TiO_4	Zn_2TiO_3	$Zn_2Ti_3O_8$	TiO_2
Z3T7	3/7	0	0	69	0	31
Z2T3-a	2/3	0	0	65	16	19
Z2T3-b	2/3	0	0	83	0	17
ZT	1/1	0	20	45	35	0
Z3T2	3/2	0	68	18	14	0
Z2T	2/1	0	100	0	0	0
Z3T	3/1	28	72	0	0	0

Table 4.1: Chemical properties of different zinc titanate sorbents [4.1]

Effects of varying the Zn/Ti atomic ratio on the physical properties of the Zn-Ti-O, that is, surface area and pore volume, are shown in figure 4.1.

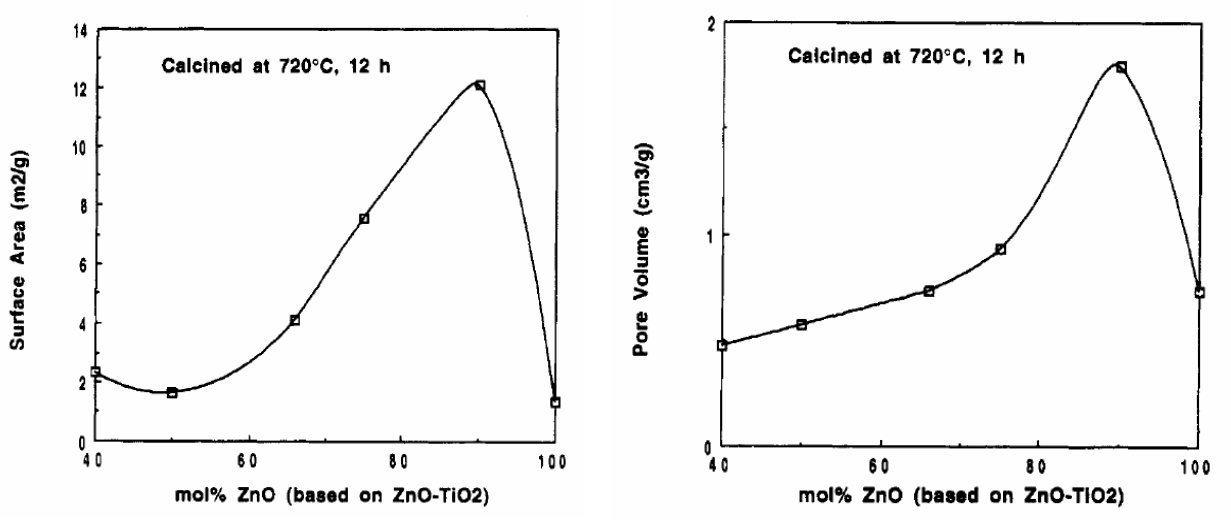

Figure 4.1: Effect of Zn-Ti-O composition on physical properties [4.2]

Solids with up to 50 mol % TiO_2 are characterized by higher surface area and pore volume than ZnO neat. Addition of small amounts of TiO_2 into ZnO has the largest effect, with a maximum in surface area and pore volume shown for $(Zn/Ti)_{atomic}$ = 9/1. These data indicate that TiO_2 disperses ZnO effectively preventing ZnO particle growth (sintering). High levels of TiO_2, however, and compound formation (e.g., $ZnTiO_3$, $Zn_2Ti_3O_8$) reduce the overall surface area [4.2].

All the sorbent zinc compounds (ZnO, Zn_2TiO_4, $ZnTiO_3$ and $Zn_2Ti_3O_8$) undergo three types of reactions: sulfidation, reduction and regeneration.

The overall reaction scheme in **sulfidation** is:

$$(1/x)Zn_xTi_yO_{x+2y}(s) + H_2S(g) \rightarrow ZnS(s) + (y/x)TiO_2(s) + H_2O(g) \qquad (Eq.\ 4.1)$$

$$(1/x)Zn_xTi_yO_{x+2y}(s) + COS(g) \rightarrow ZnS(s) + (y/x)TiO_2(s) + CO_2(g) \qquad (Eq.\ 4.2)$$

Some **reduction** can occur by the reactions:

$$(1/x)Zn_xTi_yO_{x+2y}(s) + H_2(g) \rightarrow Zn(g) + (y/x)TiO_2(s) + H_2O(g) \qquad (Eq.\ 4.3)$$

$$(1/x)Zn_xTi_yO_{x+2y}(s) + CO(g) \rightarrow Zn(g) + (y/x)TiO_2(s) + CO_2(g) \qquad (Eq.\ 4.4)$$

The **regeneration** follows the subsequent reaction:

$$ZnS(s) + (y/x)yTiO_2(s) + (3/2)O_2 \rightarrow (1/x)Zn_xTi_yO_{x+2y}(s) + SO_2(g) \qquad (Eq.\ 4.5)$$

Sulfidation experiments with pure TiO_2 found the amount of H_2S absorbed to be, in any case, negligible [4.1]. Kinetic sulfidation experiments with solids containing various Zn/Ti atomic ratios were performed in a thermo gravimetric analyzer (TGA) by Lew et al. (1989 and 1992) [4.1 and 4.2]. They reached the conclusion that the different zinc titanate phases have very similar reaction kinetics.

For example, in figure 4.2 are shown the initial sulfidation rate of the solids listed in table 4.1. The experiments in the TGA were performed under isothermal conditions, at 600ºC and 700ºC, in 2% H_2S, 1% H_2 and 97% N_2. The initial rate was similar for different zinc titanate phases despite the fact that sorbents with different Zn-Ti compositions formed different zinc titanate phases, as shown in table 4.1.

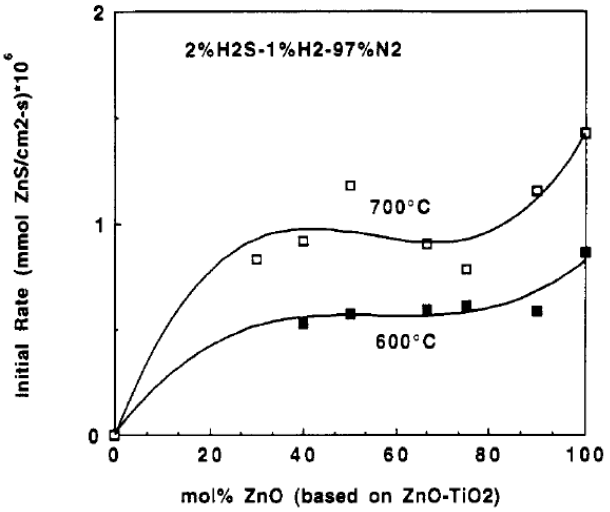

Figure 4.2: Initial sulfidation rate of several Zn-Ti-O sorbents [4.2]

Therefore, in our model we can group the Zn-Ti-O material compounds into one with the generic chemical formula $ZnTi_{\alpha}O_{(1+2\alpha)}$ which will have the same chemical behavior as any of the zinc titanate phases, since they are approximately equal. In this way, the number of equations will be reduced significantly without losing accuracy in the results.
The term α is calculated using the equation 4.6:

$$\alpha = \frac{\left(\frac{Wt\%_{Zn_2TiO_4}}{Mw_{Zn_2TiO_4}}\right)\cdot 1+\left(\frac{Wt\%_{ZnTiO_3}}{Mw_{ZnTiO_3}}\right)\cdot 1+\left(\frac{Wt\%_{Zn_2Ti_3O_8}}{Mw_{Zn_2Ti_3O_8}}\right)\cdot 3+\left(\frac{Wt\%_{TiO_2}}{Mw_{Ti_2}}\right)\cdot 1}{\left(\frac{Wt\%_{ZnO}}{Mw_{ZnO}}\right)\cdot 3+\left(\frac{Wt\%_{Zn_2TiO_4}}{Mw_{Zn_2TiO_4}}\right)\cdot 2+\left(\frac{Wt\%_{ZnTiO_3}}{Mw_{ZnTiO_3}}\right)\cdot 1+\left(\frac{Wt\%_{Zn_2Ti_3O_8}}{Mw_{Zn_2Ti_3O_8}}\right)\cdot 2} \quad (Eq.\ 4.6)$$

For instance, for the sorbent named Z3T2 (Zn/Ti atomic ratio = 1.5), which crystalline phases are: 68% Zn_2TiO_4, 18% $ZnTiO_3$ and 14% $Zn_2Ti_3O_8$ (table 4.1).

$$\alpha = \frac{\frac{68}{242.681}\cdot 1+\frac{18}{161.273}\cdot 1+\frac{14}{402.411}\cdot 3}{\frac{68}{242.681}\cdot 2+\frac{18}{161.273}\cdot 1+\frac{14}{402.411}\cdot 2} = \frac{0.2802\cdot 1+0.116\cdot 1+0.348\cdot 3}{0.2802\cdot 2+0.116\cdot 1+0.348\cdot 2} = 0.669$$

Consequently, when we will have to introduce the characteristics of the sorbent in our model, we just need to set "α = 0.669" and its generic formula will be established as: $ZnTi_{0.669}O_{(1+2\cdot 0.669)}$

B. Desulfurization & Sorbent Regeneration Reactors
The regenerable hot gas desulfurization requires two reactors:

- A **desulfurization reactor**, where the sulfidation reactions take place. In addition some reduction can also occur.

- A **sorbent regeneration reactor**, where the sulfided sorbent is carried once it leaves the first reactor. Here it is regenerated (desulfided) so it can be used again to polish the syngas.

Early reactor systems used fixed beds; however, the highly exothermic regeneration and formation of undesirable metal sulfides during regeneration promoted testing of alternative reactor designs, such as fluidized beds [4.3].
We can follow in detail the regenerable hot gas desulfurization in figure 4.3. This simplified diagram is based in on a pilot scale plant built by RTI International and Eastman Chemical Company in 2005 (figure 3.6).

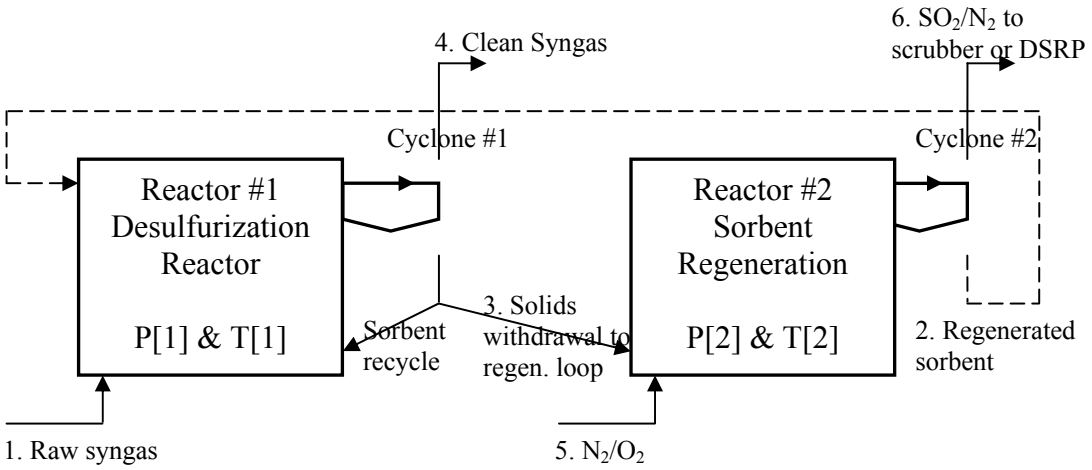

Figure 4.3: Schematic representation of regenerable syngas desulfurization [4.4]

In steady operation, a continuous flow of raw syngas and regenerated sorbent (streams #1 & #2, respectively) enter the desulfurization reactor (reactor #1).
We call "raw" the syngas leaving the gasifier. Strictly speaking, raw syngas carries small amounts of several solid compounds: C, CaO, S, SiO_2, $CaCO_3$. We shall assume that this particulate matter (ash) has been previously removed using an intermediate particulate collection system not modeled here. Nonetheless, we can find in it gaseous contaminants: COS, H_2S, SO_2, HCN and NH_3, and other usual gaseous compounds: O_2, N_2, CO_2, H_2O, H_2, CH_4 and CO.
The regenerated sorbent discharged from reactor #1 is pneumatically transported to reactor #2 and viceversa.
The raw syngas enters in contact with the sorbent and it is consequently desulfided while it goes through reactor #1. Immediately downstream of reactor #1 a cyclone device (cyclone #1) collects the particulate matter still present in the syngas to produce a clean syngas flow (stream #4) now free of sulfur compounds. This is the final product of this plant and it is ready to be used in subsequent processes.
All remaining processes sere the purpose of regenerating the exhausted sorbent so it can be reused. The solid particles captured by the cyclone #1 are then split in two flows: one is injected again into the desulfurization reactor, and the other is pneumatically transported to the sorbent regeneration reactor (reactor #2).
The regeneration reaction occurs following the injection of an oxygen stream (stream #5). Normally this oxygen is accompanied by other air components, such as N_2, CO_2, etc. Again, the gases sweep along solid sorbent particles, so they are conducted to another cyclone device (cyclone #2). The result is a particle-free flow (stream #6) which contains some sulfur dioxide as a result of the regeneration reaction, and regenerated sorbent particles that are pneumatically transported to the desulfurization reactor (stream #2), as we said before.
Finally, sulfur dioxide in stream #6 should be removed using a standard scrubbing process, or another method, such as the DSRP (not shown in figure 4.4).
We use a black box representation to help us model these interrelated processes (figure 4.4).

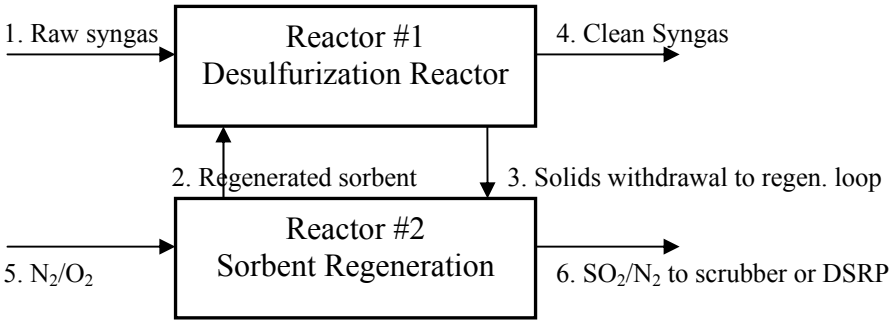

Figure 4.4: Black box representation of regenerable syngas desulfurization

In our simplified model neither the cyclone nor the pneumatic transport system are considered, because we are mainly interested in the chemical reactions and the reactors. In any case, the error introduced will be small because these are relatively small devices, which do not consume much energy and that do not change significantly the substance properties. Therefore, our regenerable syngas desulfurization model consists of two components (reactors #1 & #2) and six streams:

- There are two input streams to reactor #1: the raw syngas from the gasifier and the regenerated sorbent from the reactor #2, and other two output streams resulting from the desulfurization reactions: the sulfur free syngas and the sulfided sorbent.
- With respect to reactor #2, there are again two input streams: the reactant oxygen and the sulfided sorbent from reactor #1, and two output ones resulting from the regeneration reaction: the SO_2 rich gases and the regenerated sorbent.

C. Sulfidation Reaction

Remarkably high sulfur removal efficiencies can be achieved with the RHGD whether the operation conditions are adequately chosen and the processes are effectively controlled. For instance, in the pilot scale plant tests performed by RTI International and Eastman Chemical Company since 2005 [4.5], the clean syngas hydrogen sulfide (H_2S) concentration was reduced to a range from 0.5 to 5 ppmv. In the latest tests, the average H_2S removal efficiency was 99.97% and the average carbonyl sulfide (COS) removal efficiency was 99.96%. These data underscore the tremendous potential of this technology.

Solid conversion rate tests to determine sorbent particle conversion models were reported in two Reports by Konttinen et al. (1997) [4.6 and 4.7]. The data obtained for a sorbent with a Zn/Ti atomic ratio of 1.5 is represented in figures 4.5 and 4.6. At gasification conditions, the H_2S concentration usually ranges from 200 to 1500 ppmv, while the COS is present in a much smaller fraction. Because of that, all the efforts heading for studying the RHGD are focused on the former, because the COS will have anyway a very small influence in the desulfurization process.

The conditions of the tests were 20 bar and 650ºC, which are very close to the conditions we will find in our system. And the composition of the simulated syngas for the case of 1500 ppmv H_2S is collected in Table 4, which is also very similar to the composition of the syngas we will work with.

compd.	vol-%	compd.	vol-%
H_2	13	CH_4	2.5
CO	18	H2S	0.15
H_2O	11	N_2	balance
CO_2	8		

Table 4.2: Composition of simulated coal gas used in tests [4.7]

Figure 4.5 indicates how the zinc titanate sorbent is converted as a function of time: the mass transfer from the syngas to the sorbent is not constant, since the data points do not follow a straight line. Moreover, the curves demonstrate that the reactivity towards H_2S decreases gradually in cycling. This is an important point since sorbents would typically undergo hundreds of sulfidation-regeneration cycles in a commercial plant.

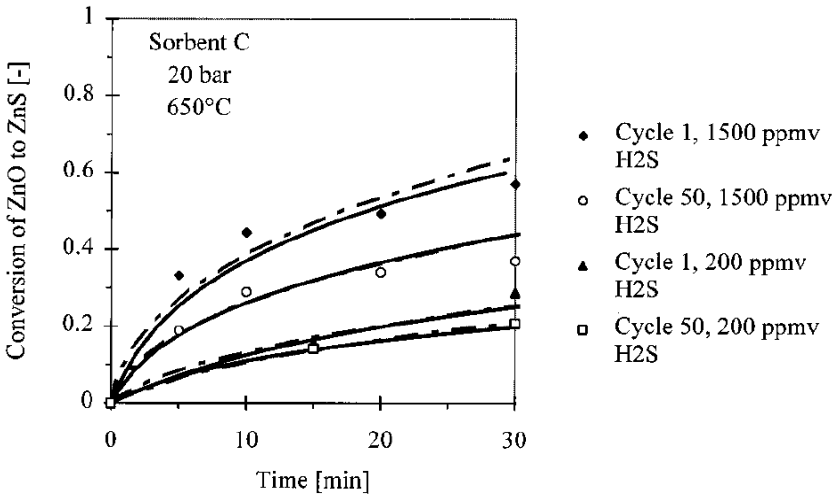

Figure 4.5: Solid conversion rate data [4.6]

From this chemical behavior follows the reactor performance in figure 4.6:

- In figure 4.5, the slope of the curve indicates the desulfurization reaction rate. Initially, with fresh sorbent, the reaction rate is high, so almost all the H_2S reacts before leaving the reactor.
- As the fresh sorbent is being sulfided, the desulfurization rate gradually decreases, so H_2S concentration in the product gas rises also little by little. This process is slow and the H_2S concentration remains at very low levels until a considerably fraction of zinc titanate sorbent has reacted.
- At a certain fractional sorbent conversion value, the slope in figure 4.6 changes abruptly and it starts rising rapidly. This point is called the breakthrough. What happens is that the decrease in reactive sorbent has slowed down too much the desulfurization rate, and a high percentage of H_2S leaves the reactor without reacting.

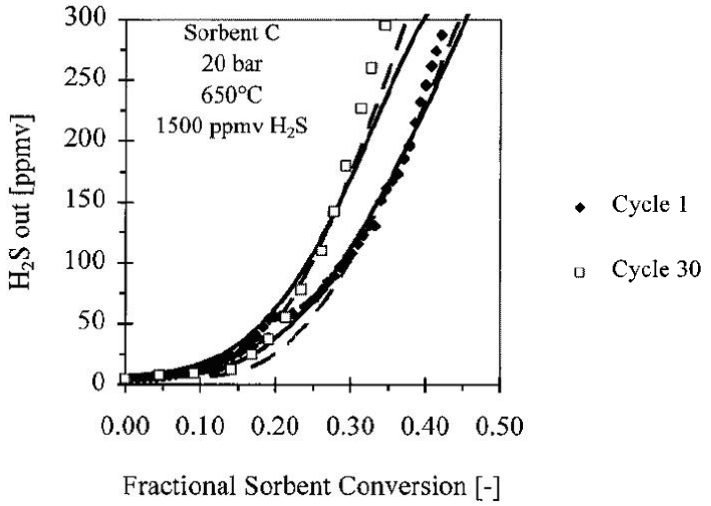

Figure 4.6: Fluidized bed sulfidation data [4.7]

We can use the same data used to draw the previous figure to draw desulfurization efficiency as a function of fractional sorbent conversion (figure 4.7). In particular, we are using the data from the cycle no. 30, that represent a sufficiently close description of the average behavior of the sorbent over all the cycles the sorbent will undergo in a commercial plant.

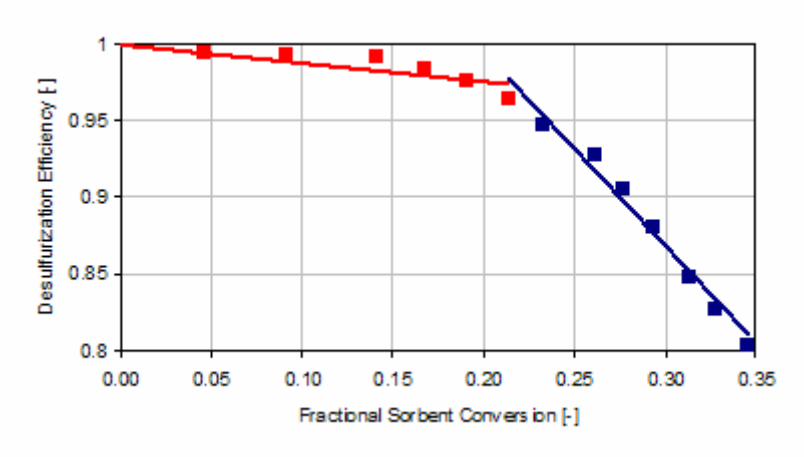

Figure 4.7: Fluidized bed desulfurization efficiency

Qualitatively speaking, for high sulfur removal efficiency, a sufficiently large amount of sorbent must be reactive inside the reactor, that is, the fractional conversion must be low. Accomplishing this entails transporting a high mass flowrate of sorbent per unit of time to the regeneration sorbent reactor. On the contrary, for low sulfur removal efficiency, a smaller amount of the sorbent has to be reactive inside the reactor, that is, the fractional conversion can be higher, and the mass flowrate of the sorbent being regenerated is lower.

By fitting the data points in figure 4.7 with two lineal expressions, one before the breakthrough and the other after it, we obtain:

$$y = \begin{cases} -0.123x + 1 & 0 \le x \le 0.20 \\ -1.350x + 1.2454 & 0.20 \le x \le 0.35 \end{cases} \qquad (Eq.\ 4.7)$$

The tendency of the data indicates that, for this case, the breakthrough point is at 0.20 fractional solid conversion. The slope of the adjusted line for the points before the breakthrough is notably smaller than the corresponding to the data after it, as we were expecting.

We will use equation 4.7 to calculate the average fractional sorbent conversion that, at steady state, the sorbent should maintain inside the desulfurization reactor for a desulfurization efficiency defined by the user. This expression is correct for a system at the same conditions as the experiment, but we will assume that it is also valid for our model since the simulation conditions: pressure, temperature, syngas composition, sorbent, etc., will be very close to the former, and the characteristics of the reactor (sorbent mass, syngas space velocity, etc.) would be scaled up for the syngas flow the system will have to polish.

For all these reasons, we think the equation 4.7 is a good first step to simulate the desulfurization reactor component. Further study about how this equation varies with the process parameters is not discussed here, since it is beyond the scope of this work.

COS is present in a much smaller fraction than H_2S, so its influence in the desulfurization process is very small. So, we will simply assume that its removal efficiency is equal to the one of the H_2S. This is also correct according to the available information [4.5].

Since different crystalline structures of the zinc titanate can be formed, a practical simplification is to assume that ZnO be the reactive solid. Thus, the overall reaction scheme in **sulfidation** is:

$$ZnO(s) + H_2S(g) \rightarrow ZnS(s) + H_2O(g) \quad (Eq.\ 4.8)$$

$$ZnO(s) + COS(g) \rightarrow ZnS(s) + CO_2(g) \quad (Eq.\ 4.9)$$

The gaseous compounds H_2 and CO can decrease the amount of reactive zinc during sulfidation through **reduction** reactions:

$$ZnO(s) + H_2(g) \rightarrow Zn(g) + H_2O(g) \quad (Eq.\ 4.10)$$

$$ZnO(s) + CO(g) \rightarrow Zn(g) + CO_2(g) \quad (Eq.\ 4.11)$$

However, Lew et al. (1992) [4.2] observed no effects of these compounds on sulfidation kinetics. On this basis, it is assumed here that the relative contribution of sorbent reduction to the rate of sulfidation is insignificant.

Titanium dioxide is not a reactive component, but its mission is to stabilize the ZnO. So, it does not intervene directly in the chemical reactions, but since both are linked to the ZnO and ZnS, they constitute

a mass that also has to be transported between the reactors. We will use the variable α, defined in equation 4.6, to estimate this.

D. Sorbent Regeneration Reaction

After sulfidation of the sorbent to a certain predetermined level, the sorbent is regenerated. The desirable reaction in zinc titanate regeneration is:

$$ZnS(s) + (3/2)O_2 \rightarrow ZnO(s) + SO_2(g) \qquad (Eq.\ 4.12)$$

The individual oxides of the sorbent are then assumed to produce the original zinc titanium oxide starting material as follows:

$$xZnO(s) + yTiO_2 \rightarrow Zn_xTi_yO_{(x+2y)} \qquad (Eq.\ 4.13)$$

At regeneration conditions, undesired zinc sulfate can however be formed via secondary reactions with freshly formed ZnO, such as:

$$ZnO(s) + SO_2 + (1/2)O_2 \rightarrow ZnSO_4(s) \qquad (Eq.\ 4.14)$$

Figure 4.8 shows the phase diagram of the Zn-O-S system as a function of O_2 and SO_2 partial pressures. At the relevant temperature range of the regeneration reactor (500-750 °C), the phase diagram suggests that the regeneration of sulfided zinc titanate according to equation 4.12 is possible by using a combination of low O_2 and SO_2 partial pressures.

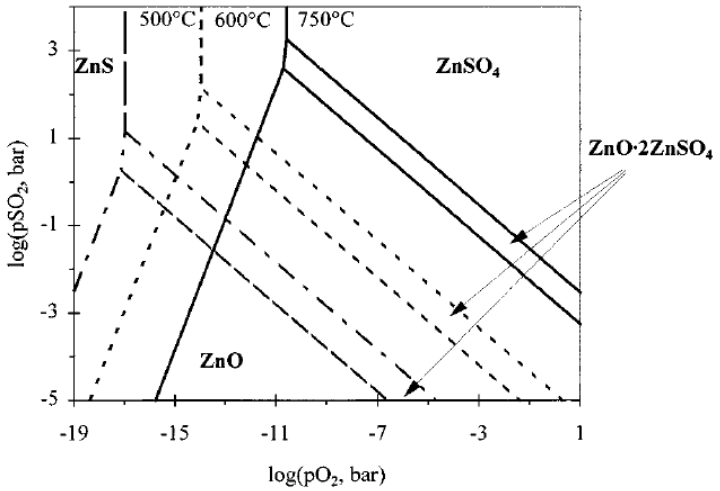

Figure 4.8: Zn-O-S phase stability diagram [4.8]

As a rule of thumb, the partial pressure of O_2 in the inlet gas used in the sorbent regeneration reaction (stream # 5 in figure 4.4) should not exceed 0.6 bar, to avoid the formation of zinc sulfates [4.9]. For instance, if our regeneration reactor works at 20 bar, according to this criterion the limit of O_2 should be 3% in volume. The easiest form to obtain the desired inlet gas composition is through mixing ambient air and nitrogen (table 4.3).

compd.	Ambient air [vol-%]	Nitrogen [vol-%]	Inlet gas [vol-%]	Inlet gas [mass-%]
O_2	20.59	0	3	3.4152
N_2	77.48	100	96.7188	96.4005
CO_2	0.03	0	0.0044	0.0069
H_2O	1.9	0	0.2768	0.1775

Table 4.3: Composition of inlet gas for 20 bar regeneration reactor pressure

$$x_{ambient\_air} = \frac{3}{20.59} = 0.1457;\ x_{N_2} = 1 - x_{ambient\_air} = 1 - 0.1457 = 0.8543$$

We will use this approach in our model to determine the inlet gas composition to the sorbent regeneration reactor.

Several experimental results of conversion of sulfided zinc titanate to zinc oxide are shown in figure 4.9. Regeneration can achieve 100% efficiency with enough residential time, and at high pressure and temperature conditions.
Since our reactor will also work at high pressure and temperature conditions, as shown in figure 4.9 for sorbent D, we will suppose that the reactor and inlet gas flow will be designed to allow enough residential time to accomplish a 100% sorbent regeneration.

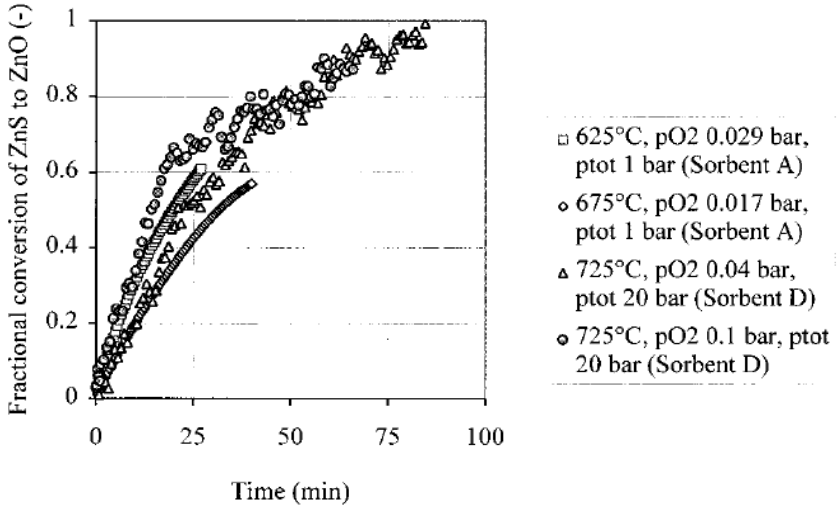

Figure 4.9: Comparison of time vs sulfided zinc titanate conversion data [4.9]

Much more detailed information about sorbent regeneration kinetics and reactor design can be found in several Reports published by Konttinen et al. (1997) [4.9 and 4.10]. But we will not continue discussing this topic, since we consider it would be beyond the scope of this study
At usual temperature, pressure and $\%O_2$ inlet gas conditions, experiments yielded much lower reaction rates for zinc sulfate formation reactions than for regeneration reactions. For example, in one of the regeneration experiments performed by Konttinen et al. (1997) [4.9], at 650 ºC, 20 bar and 3 vol-% O_2, the reaction sulfate formation rates (equation 4.14) were about $3 \cdot 10^{-5}$ [1/s], while the sulfided zinc titanate regeneration rates were in the order of $5 \cdot 10^{-3}$ [1/s], which is about two orders of magnitude higher. This comparison indicates that the relative contribution of sulfate formation is insignificant, so we will not take it into account in our model.

E. Direct Sulfur Recovery Process (DSRP)
Regeneration of the sulfided sorbent using oxygen containing gas stream results in a sulfur dioxide containing off-gas at high pressure and high temperature conditions. A patented Direct Sulfur Recovery Process (DSRP), developed by Research Triangle Institute (RTI) is a highly attractive option for recovery of sulfur from this regeneration off-gas. Using a slipstream of coal gas as a reducing agent, it efficiently converts the SO_2 to elemental sulfur, an essential industrial commodity that is easily stored and transported [4.11].
The sulfur dioxide containing off-gas is reacted with a slipstream of coal gas over a fixed bed of a selective catalyst to directly produce elemental sulfur. Overall reactions involved are shown below:

$$2H_2 + SO_2 \rightarrow (1/n)S_n + 2H_2O \qquad (Eq.\ 4.15)$$

$$2CO + SO_2 \rightarrow (1/n)S_n + 2CO_2 \qquad (Eq.\ 4.16)$$

$$CO + H_2O \rightarrow H_2 + CO_2 \qquad (Eq.\ 4.17)$$

$$H_2 + (1/n)S_n \rightarrow H_2S \qquad (Eq.\ 4.18)$$

$$2H_2S + SO_2 \rightarrow (3/n)S_n + 2H_2O \qquad (Eq.\ 4.19)$$

One of the options to integrate the DSRP with the metal oxide sorbent regenerator is shown in figure 4.10. There is a potential for "zero" sulfur emissions if the DSRP tail gas is recycled, as shown in figure 3.21.

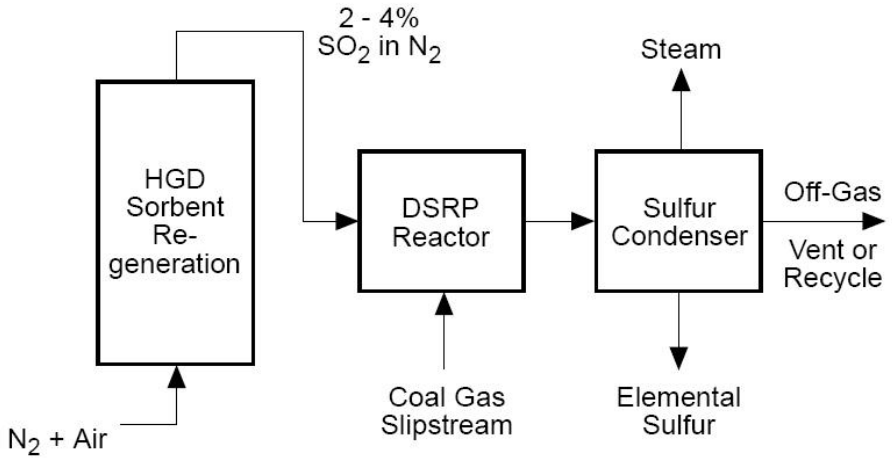

Figure 4.10: DSRP integration in sorbent regeneration [4.11]

Slipstream tests with actual coal gas demonstrated that, with careful control of the stoichiometric ratio of the gas input, an adequate catalyst, and favorable pressure and temperature conditions, sulfur recovery of 96 to 98 percent can be consistently achieved in a DSRP [4.12].

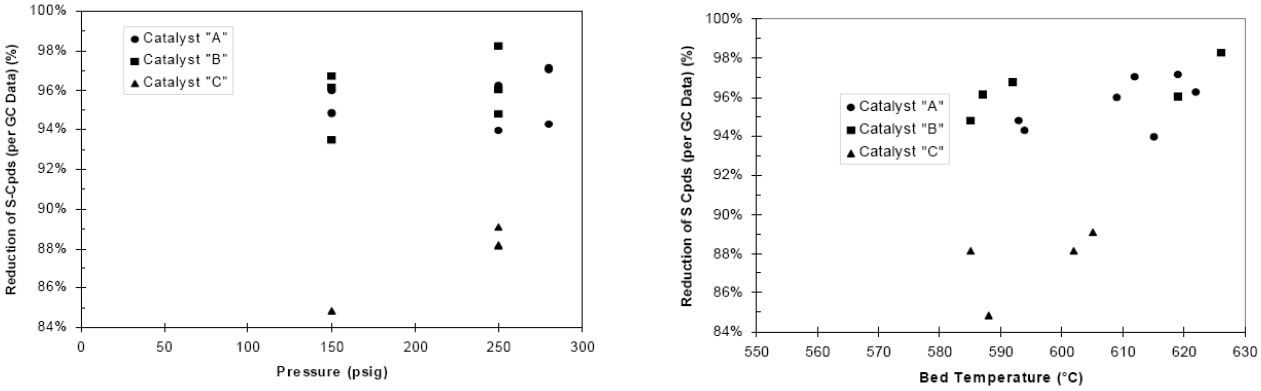

Figure 4.11: Effects of pressure and bed temperature [4.12]

Furthermore, DSRP has undergone long field testing at gasifier sites, like the 800 hours Eastman Field Test in October 2005, with successful results. And independent economic evaluations show DSRP to cost about a fourth of competing technologies, such as Claus-SCOT process [4.13]. So we consider it worthy of being integrated in our RHGD plant, because it is a technology with a big potential that can be commercially available in a short term period.
Using the RHGD black box representation in figure 4.4 as a base, we add the DSRP component (figure 4.12).

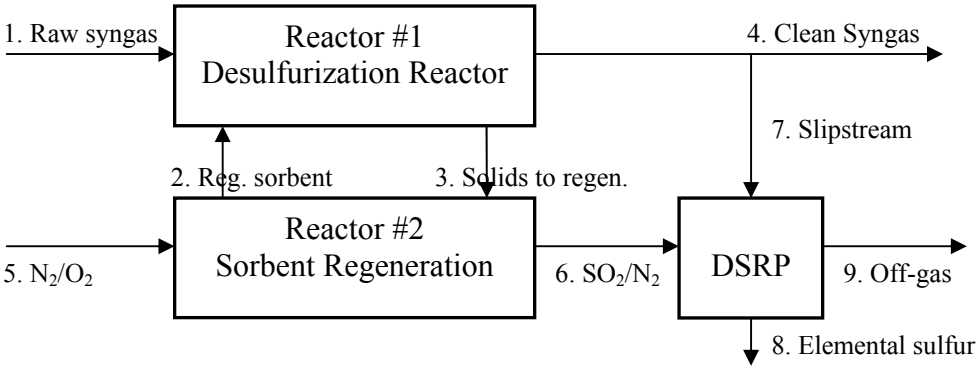

Figure 4.12: Black box representation of regenerable syngas desulfurization

There are two input stream: the sulfur dioxide containing off-gas from reactor #2 (stream #6), and the slipstream of clean syngas (stream #7) that will act as the reducing agent. The DSRP occurs at high pressure and temperature. As a reference we can use 15 bar and 620 ºC, based on the field test parameters. With an adequate catalyst and reactor design, the efficiency is usually very high, in the range from 96 to 98 %. When the sulfur dioxide reacts with the slipstream of coal, it is produced elemental sulfur (stream #8) which is separated from the rest of the off-gas (stream #9).

4.2 The Governing Equations

The equations that model the desulfurization and regeneration processes are listed in Appendix 1. They have been divided into four groups:

- Mass balance equations that relate the mass flows and compound weight fractions of the output streams, the input streams and some system parameters.
- Thermodynamic equations that provide the specific enthalpy of formation, the specific enthalpy, the specific entropy and the specific exergy of any stream as a function of its composition, its pressure, its temperature, and the reference pressure and temperature.
- Heat flow equations that calculate Q_{lost} (heat lost due to a non perfect thermal insulation), and Qi (input heat from an external source) as result of the energy balance.
- Exergy equations that compute the destroyed exergy and the exergetic efficiency of the process.

a) Unknowns

The unknowns associated to each stream type are:

Syngas (S)		**Sorbent (Z)**	**Air (Z)**	
m	x_{H2O}	m	m	x_{H2O}
p	x_{H2}	p	p	
T	x_{CH4}	T	T	
hf	x_{CO}	hf	hf	
h	x_{COS}	h	h	
s	x_{H2S}	s	s	
ex	x_{SO2}	ex	ex	
x_{O2}	x_{HCN}	x_{ZnO}	x_{O2}	
x_{N2}	x_{NH3}	x_{ZnS}	x_{N2}	
x_{CO2}		x_{TiO2}	x_{CO2}	

Table 1: Unknowns associated to each stream type

Desulfuration Reactor

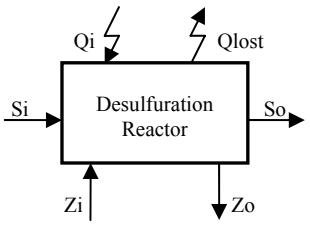

Figure 4.13: Desulfuration reactor black-box representation

Mass balance equations:

$$\left[\dot{m}\cdot x_{O_2}\right]_{So} = \left[\dot{m}\cdot x_{O_2}\right]_{Si} \quad (1)$$

$$\left[\dot{m}\cdot x_{N_2}\right]_{So} = \left[\dot{m}\cdot x_{N_2}\right]_{Si} \quad (2)$$

$$\left[\dot{m}\cdot x_{CO_2}\right]_{So} = \left[\dot{m}\cdot x_{CO_2}\right]_{Si} \quad (3)$$

$$\left[\dot{m}\cdot x_{H_2O}\right]_{So} = \left[\dot{m}\cdot x_{H_2O}\right]_{Si} + Eff\,\frac{Mw_{H_2O}}{Mw_{H_2S}}\left[\dot{m}\cdot x_{H_2S}\right]_{Si} \quad (4)$$

$$\left[\dot{m}\cdot x_{H_2}\right]_{So}=\left[\dot{m}\cdot x_{H_2}\right]_{Si} \quad (5)$$

$$\left[\dot{m}\cdot x_{CH_4}\right]_{So}=\left[\dot{m}\cdot x_{CH_4}\right]_{Si} \quad (6)$$

$$\left[\dot{m}\cdot x_{CO}\right]_{So}=\left[\dot{m}\cdot x_{CO}\right]_{Si} \quad (7)$$

$$\left[\dot{m}\cdot x_{COS}\right]_{So}=\left[\dot{m}\cdot x_{COS}\right]_{Si} \quad (8)$$

$$\left[\dot{m}\cdot x_{H_2S}\right]_{So}=\left[\dot{m}\cdot x_{H_2S}\right]_{Si}\left(1-Eff\right) \quad (9)$$

$$\left[\dot{m}\cdot x_{SO_2}\right]_{So}=\left[\dot{m}\cdot x_{SO_2}\right]_{Si} \quad (10)$$

$$\left[\dot{m}\cdot x_{HCN}\right]_{So}=\left[\dot{m}\cdot x_{HCN}\right]_{Si} \quad (11)$$

$$\left[\dot{m}\cdot x_{NH_3}\right]_{So}=\left[\dot{m}\cdot x_{NH_3}\right]_{Si} \quad (12)$$

$$\sum_{\forall i}\left[x_i\right]_{So}=1 \quad (13)$$

$$\frac{\left[x_{ZnO}\right]_{Zo}}{Mw_{ZnO}}=\frac{\left[x_{ZnS}\right]_{Zo}}{Mw_{ZnS}}\frac{\left(1-x\right)}{x} \quad (14)$$

$$\left[\dot{m}\cdot x_{ZnS}\right]_{Zo}=Eff\,\frac{Mw_{ZnS}}{Mw_{H_2S}}\left[\dot{m}\cdot x_{H_2S}\right]_{Si} \quad (15)$$

$$\frac{\left[x_{TiO_2}\right]_{Zo}}{Mw_{TiO_2}}=\alpha\left(\frac{\left[x_{ZnS}\right]_{Zo}}{Mw_{ZnS}}+\frac{\left[x_{ZnO}\right]_{Zo}}{Mw_{ZnO}}\right) \quad (16)$$

$$\left[x_{ZnO}+x_{ZnS}+x_{TiO_2}\right]_{Zo}=1 \quad (17)$$

Thermodynamic equations:

$$hf_{Si}=EnthFormGas\left(\left[x_i\right]_{Si}\right) \quad (18)$$

$$p_{So}=p_r \quad (19)$$

$$T_{So}=T_r \quad (20)$$

$$h_{So}=EnthGas\left(\left[x_i\right]_{So},T_{So},p_{So}\right) \quad (21)$$

$$s_{So}=EntrGas\left(\left[x_i\right]_{So},T_{So},p_{So}\right) \quad (22)$$

$$ex_{So}=ExeGas\left(\left[x_i\right]_{So},T_{So},p_{So},T_{ref},p_{ref}\right)_{So} \quad (23)$$

$$hf_{So}=EnthFormGas\left(\left[x_i\right]_{So}\right) \quad (24)$$

$$hf_{Zi}=EnthFormSorbent\left(\left[x_i\right]_{Zi}\right) \quad (25)$$

$$p_{Zo}=p_r \quad (26)$$

$$T_{Zo}=T_r \quad (27)$$

$$h_{Zo}=EnthSorbent\left(\left[x_i\right]_{Zo},T_{Zo},p_{Zo}\right) \quad (28)$$

$$s_{Zo}=EntrSorbent\left(\left[x_i\right]_{Zo},T_{Zo},p_{Zo}\right) \quad (29)$$

$$ex_{Zo}=ExeSorbent\left(\left[x_i\right]_{Zo},T_{Zo},p_{Zo},T_{ref},p_{ref}\right) \quad (30)$$

$$hf_{Zo}=EnthFormSorbent\left(\left[x_i\right]_{Zo}\right) \quad (31)$$

Heat flow equations:

$$Q_{lost}=Q_l\left(\left[\dot{m}\cdot h\right]_{Si}+\left[\dot{m}\cdot h\right]_{Zi}\right) \quad (32)$$

$$\sum_{j=Si,Zi}\left[\dot{m}\left(h+hf\right)\right]_j+Qi=\sum_{j=So,Zo}\left[\dot{m}\left(h+hf\right)\right]_j+Q_{lost} \quad (33)$$

Exergy balance equations:

$$ExD = \sum_{j=Si,Zi} \left[\dot{m} \cdot ex\right]_j - \sum_{j=So,Zo} \left[\dot{m} \cdot ex\right]_j + Qi\left(1 - \frac{T_{ref}}{Tr}\right) \quad (34)$$

$$if\ \left(Qi \geq 0\right)\ ExEff = \frac{\left[\dot{m} \cdot ex\right]_{So} + \left[\dot{m} \cdot ex\right]_{Zo}}{\left[\dot{m} \cdot ex\right]_{Si} + \left[\dot{m} \cdot ex\right]_{Zi} + Qi\left(1 - \frac{T_{ref}}{Tr}\right)} \quad (35)$$

$$if\ \left(Qi < 0\right)\ ExEff = \frac{\left[\dot{m} \cdot ex\right]_{So} + \left[\dot{m} \cdot ex\right]_{Zo} - Qi\left(1 - \frac{T_{ref}}{Tr}\right)}{\left[\dot{m} \cdot ex\right]_{Si} + \left[\dot{m} \cdot ex\right]_{Zi}} \quad (35')$$

Reactor steady point:

$$Eff = \begin{cases} -0.12x + 1.00 & 0 \leq x \leq 0.20 \\ -1.35x + 1.25 & 0.20 \leq x \leq 0.35 \end{cases} \quad (36)$$

Equation 36 is just an example. It is only strictly valid for the particular conditions under which it was obtained: temperature, pressure, gas flow rate, mass of sorbent, H_2S concentration, type of sorbent, etc.
A method to calculate other equations for new operating conditions has been developed and is currently under testing, but it does not fall within the scope of the present Report.

Regeneration Reactor

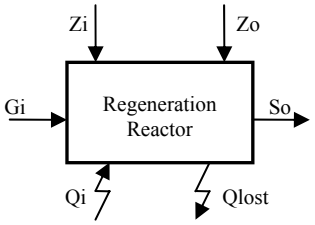

Figure 4.14: Regeneration reactor black-box representation

Mass balance equations:

$$\left[\dot{m} \cdot x_{O_2}\right]_{So} = \left[\dot{m} \cdot x_{O_2}\right]_{Gi} - 1.5 \cdot Eff_{Reg} \frac{Mw_{O_2}}{Mw_{ZnS}} \left[\dot{m} \cdot x_{ZnS}\right]_{Zi} \quad (37)$$

$$\left[\dot{m} \cdot x_{N_2}\right]_{So} = \left[\dot{m} \cdot x_{N_2}\right]_{Gi} \quad (38)$$

$$\left[\dot{m} \cdot x_{CO_2}\right]_{So} = \left[\dot{m} \cdot x_{CO_2}\right]_{Gi} \quad (39)$$

$$\left[\dot{m} \cdot x_{H_2O}\right]_{So} = \left[\dot{m} \cdot x_{H_2O}\right]_{Gi} \quad (40)$$

$$\left[x_{H_2}\right]_{So} = 0 \quad (41)$$

$$\left[x_{CH_4}\right]_{So} = 0 \quad (42)$$

$$\left[x_{CO}\right]_{So} = 0 \quad (43)$$

$$\left[x_{COS}\right] = 0 \quad (44)$$

$$\left[x_{H_2S}\right]_{So} = 0 \quad (45)$$

$$\left[\dot{m} \cdot x_{SO_2}\right]_{So} = Eff_{Reg} \frac{Mw_{SO_2}}{Mw_{ZnS}} \left[\dot{m} \cdot x_{ZnS}\right]_{Zi} \quad (46)$$

$$\left[x_{HCN}\right]_{So} = 0 \quad (47)$$

$$\left[x_{NH_3}\right]_{So} = 0 \quad (48)$$

$$\sum_{\forall i}\left[x_i\right]_{So} = 1 \tag{49}$$

$$\left[\dot{m}\cdot x_{ZnO}\right]_{Zo} = \left[\dot{m}\cdot x_{ZnO}\right]_{Zi} + Eff_{Reg}\,\frac{Mw_{ZnO}}{Mw_{ZnS}}\left[\dot{m}\cdot x_{ZnS}\right]_{Zi} \tag{50}$$

$$\left[\dot{m}\cdot x_{ZnS}\right]_{Zo} = \left(1-Eff_{Reg}\right)\left[\dot{m}\cdot x_{ZnS}\right]_{Zi} \tag{51}$$

$$\left[\dot{m}\cdot x_{TiO_2}\right]_{Zo} = \left[\dot{m}\cdot x_{TiO_2}\right]_{Zi} \tag{52}$$

$$\left[x_{ZnO} + x_{ZnS} + x_{TiO_2}\right]_{Zo} = 1 \tag{53}$$

Thermodynamic equations:

$$hf_{Gi} = EnthFormGas\left(\left[x_i\right]_{Gi}\right) \tag{54}$$

$$p_{So} = p_r \tag{55}$$

$$T_{So} = T_r \tag{56}$$

$$h_{So} = EnthGas\left(\left[x_i\right]_{So}, T_{So}, p_{So}\right) \tag{57}$$

$$s_{So} = EntrGas\left(\left[x_i\right]_{So}, T_{So}, p_{So}\right) \tag{58}$$

$$ex_{So} = ExeGas\left(\left[x_i\right]_{So}, T_{So}, p_{So}, T_{ref}, p_{ref}\right)_{So} \tag{59}$$

$$hf_{So} = EnthFormGas\left(\left[x_i\right]_{So}\right) \tag{60}$$

$$hf_{Zi} = EnthFormSorbent\left(\left[x_i\right]_{Zi}\right) \tag{61}$$

$$p_{Zo} = p_r \tag{62}$$

$$T_{Zo} = T_r \tag{63}$$

$$h_{Zo} = EnthSorbent\left(\left[x_i\right]_{Zo}, T_{Zo}, p_{Zo}\right) \tag{64}$$

$$s_{Zo} = EntrSorbent\left(\left[x_i\right]_{Zo}, T_{Zo}, p_{Zo}\right) \tag{65}$$

$$ex_{Zo} = ExeSorbent\left(\left[x_i\right]_{Zo}, T_{Zo}, p_{Zo}, T_{ref}, p_{ref}\right) \tag{66}$$

$$hf_{Zo} = EnthFormSorbent\left(\left[x_i\right]_{Zo}\right) \tag{67}$$

Heat flow equations:

$$Q_{lost} = Q_l\left(\left[\dot{m}\cdot h\right]_{Si} + \left[\dot{m}\cdot h\right]_{Zi}\right) \tag{68}$$

$$\sum_{j=Gi,Zi}\left[\dot{m}\left(h+hf\right)\right]_j + Qi = \sum_{j=So,Zo}\left[\dot{m}\left(h+hf\right)\right]_j + Q_{lost} \tag{69}$$

Exergy balance equations:

$$ExD = \sum_{j=Gi,Zi}\left[\dot{m}\cdot ex\right]_j - \sum_{j=So,Zo}\left[\dot{m}\cdot ex\right]_j + Qi\left(1-\frac{T_{ref}}{Tr}\right) \tag{70}$$

$$if\ \left(Qi \ge 0\right)\ ExEff = \frac{\left[\dot{m}\cdot ex\right]_{So} + \left[\dot{m}\cdot ex\right]_{Zo}}{\left[\dot{m}\cdot ex\right]_{Si} + \left[\dot{m}\cdot ex\right]_{Zi} + Qi\left(1-\frac{T_{ref}}{Tr}\right)} \tag{71}$$

$$if\ \left(Qi < 0\right)\ ExEff = \frac{\left[\dot{m}\cdot ex\right]_{So} + \left[\dot{m}\cdot ex\right]_{Zo} - Qi\left(1-\frac{T_{ref}}{Tr}\right)}{\left[\dot{m}\cdot ex\right]_{Si} + \left[\dot{m}\cdot ex\right]_{Zi}} \tag{72}$$

SECTION 5 - CODING IN CAMEL

CAMEL is a simulation software for thermal processes developed by the Department of Mechanical and Aeronautical of the University of "La Sapienza". This package was used to simulate the regenerative HTHPD model: in this way, we were able to integrate the HPHTD into the ZECOMIX process, also under assessment at the same Department within the frame of an ENEA (the Italian Energy Agency) International Project.

The ZECOMIX plant is a special type of IGCC, where H_2-rich syngas is produced by coal hydrogasification and CO_2 capture processes, and then used to fuel an unconventional steam-based combined cycle, ZECOTECH©.

The ZECOMIX gasifier is modeled in CAMEL as shown in figure 8. The original process scheme simply assumed that the gaseous contaminants were separated from the rest of the syngas, with no energy consumption.

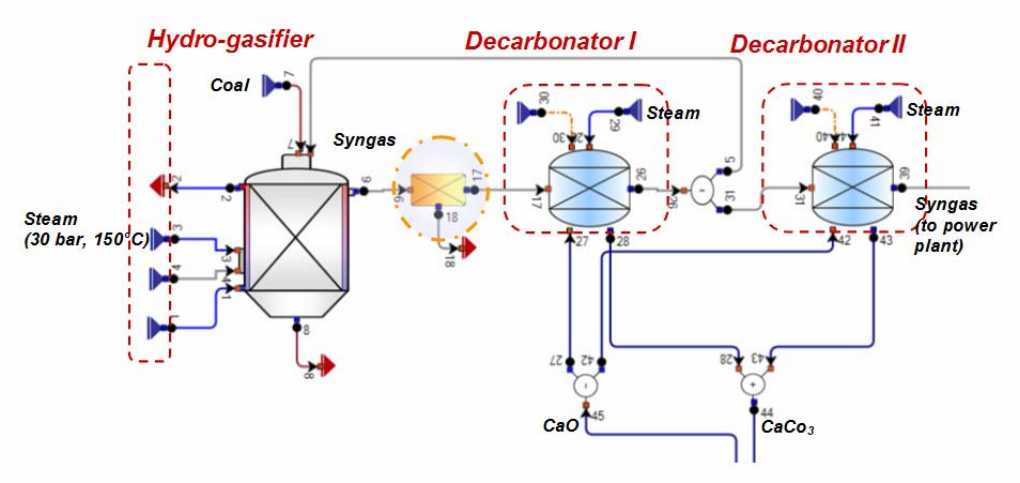

Figure 5.1: Gasifier w/o regenerative HTHPD

Figure 9 shows the resulting configuration after the regenerative HTHPD system was integrated into the ZECOMIX gasifier.

The HTHPD system is composed of tree components: a desulfuration reactor, a sorbent regeneration reactor and a compressor.

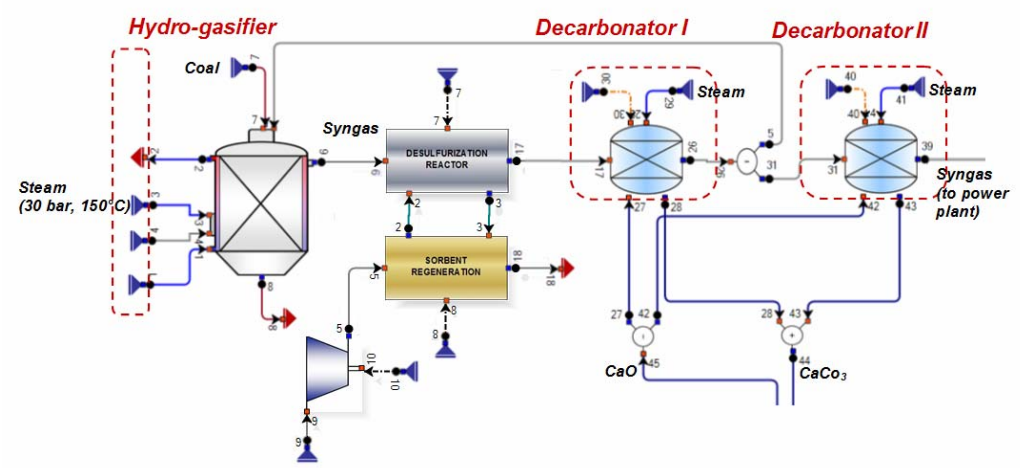

Figure 5.2: Gasifier with regenerative HTHPD

SECTION 6 – SIMULATION RESULTS

Once the regenerative HTHPD system was integrated in CAMEL, a series of simulations of the complete process was performed. To facilitate the comparison between the configuration "with" and "without" the HTHPD, several variables were aSsigned as input data:

1- Both the syngas composition (Table 1) and the mass flow rate (3.69 kg/s) duplicate the stream produced by the hydrogasifier in the original ZECOMIX plant (25 MWe).

H_2	7.06%	O_2	0.00%	H_2O	63.91%
CH_4	15.78%	HCN	0.00%	Cl_2	0.00%
CO_2	7.66%	COS	0.00%	S	0.00%
CO	3.32%	H_2S	0.36%	SiO_2	1.12%
C	0.00%	HCl	0.05%		
N_2	0.71%	NH_3	0.04%		

Table 1: Syngas mass composition (Amati et al. [13])

2 - The desulfuration and regeneration reactors operate at the same pressure in both configurations.

3 - The presence of O_2 in the gas used for regeneration is limited to 0.6 bar to avoid the formation of zinc sulfates, as was indicated by Konttinen et al. [10].

4 - The regeneration reactor is adiabatic.

5- The zinc-titanate sorbent is the same as that tested by Konttinen et al. [5]. The reactor performance maps have been calculated with the reactor model presented in Section 3.

6.1 - Destroyed Exergy Allocation

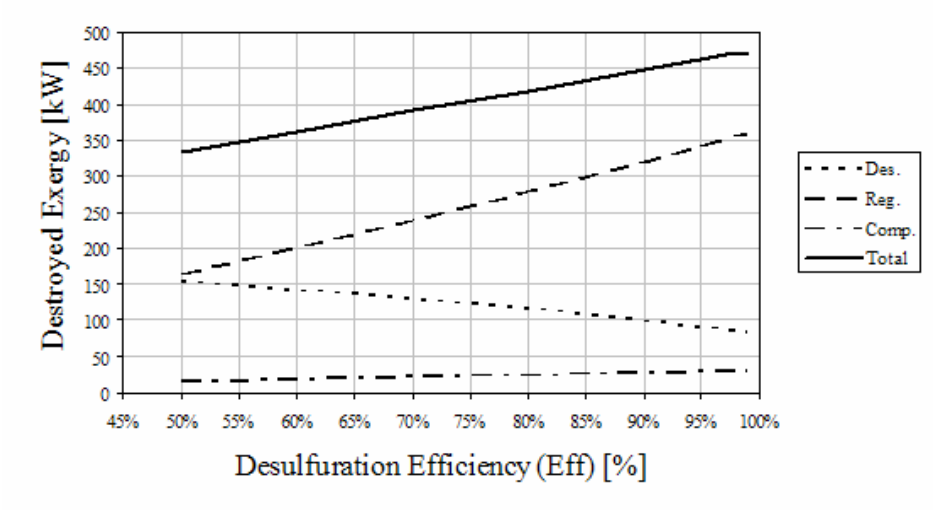

Figure 6.1: Destroyed exergy vs. removal efficiency

The total destroyed exergy in the process increases almost linearly with the desulfuration efficiency. Its behaviour is opposite in the desulfuration and regeneration reactors: in the former, a higher desulfuration efficiency leads to a lower exergy destruction, while the opposite is true for the regenerator. For its part, the destroyed exergy in the compressor is proportional to its efficiency and, since the pressure ratio is fixed, to the N_2+O_2 mass flow rate required by sorbent regeneration.

Figure 10 shows the simulation results for a desulfuration process at 30 bar and 700ºC.

6.2 - Specific Exergy Destruction

The destroyed exergy per unit mass of H_2S removed decreases almost hyperbolically as desulfuration efficiency increases. Figure 11 shows the results of a series of simulations for a desulfuration process at 30 bar, with temperatures between 500 and 750 ºC. In this case, the minimum is achieved at 700 ºC. A more detailed analysis revealed that the process as a whole is almost adiabatic (exo- and endothermal reactions balance out) at this temperature.

The behavior is qualitatively equivalent for other operating conditions, and in all examined cases the exergy destruction per amount of H_2S removed is minimized at adiabatic conditions.

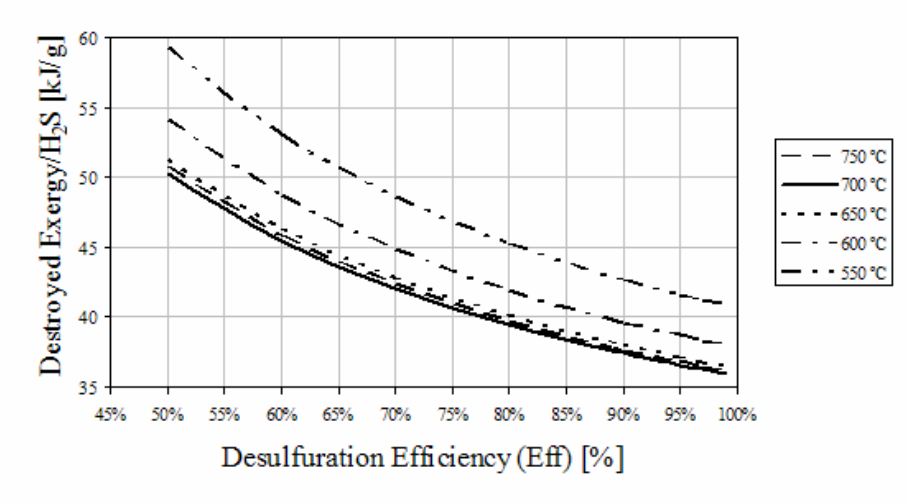

Figure 6.2: Specific destroyed exergy

6.3 - Sorbent Mass Flow

The amount of sorbent that must be transported between reactors depends on the desired desulfurization efficiency, on the amount of sorbent in the reactor, and on the operating pressure and temperature.

To higher desulfuration efficiencies correspond lower fractions of sorbent sulfided in the reactor, and consequently higher flows of sorbent to be regenerated. This tendency can be observed in Fig. 12.

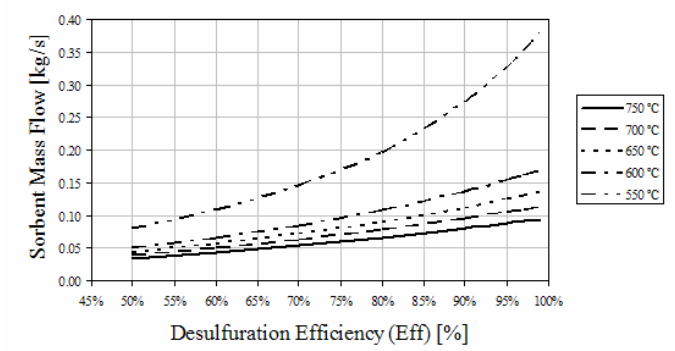

Figure 6.3: Sorbent mass flowrate – 30 bar, 500 kg.

It is also known that sorbent is more efficiently used at higher temperatures, which amplify both the gas molecular diffusion and the chemical reaction rate. The conclusion drawn from the simulation results is that this influence is very strong, especially at high desulfurations efficiencies.

6.4 - Adiabatic Desulfuration

The reactor temperature for an adiabatic desulfuration process is, basically, a function of syngas temperature. The influence of other parameters, such as desulfurization efficiency and pressure, is almost negligible.

6.5 – Integration into ZECOMIX

Several alternative configurations of the ZECOMIX plant have been analysed in other Reports [reff. Nostre], to which readers are referred for more detailed information: here, we present some of the most interesting and useful results we obtained by integrating the regenerative HTHPD model into a ZECOMIX process model. The syngas enters the HTHPD at 991 K and 30 bar, and its composition is reported in Table 1.

- If the desulfuration process is adiabatic and at steady state, the desulfuration and regeneration reactor operate respectively at 700 ºC and 740 ºC.

- The amount of sorbent required in the desulfuration reactor for a proper operation was estimated in 500 kg.

- Once the regenerative HTHPD is integrated into the whole ZECOMIX plant, some process variables do not vary even if the HTHPD operating conditions change, such as the reactor temperatures and the reactor heat lost.

- Others, such as the sorbent mass flow (the amount of sorbent that must be transported between reactors to be regenerated) are strongly affected by the amount of sorbent present in the reactor (m_{sorb}). For example, a 25% reduction in the second variable implied a 16% increment in the first one. Consequently, the designer should estimate the most convenient configuration.

- The energy needed to power the compressor is 37 kJ per gram of H_2S removed. This implies 467 kW for 95% desulfuration efficiency in the prototype ZECOMIX plant, i.e., in relative terms, the exergetic penalty for the HTHPD addition amounts to 1.86% of the generated electricity.

SECTION 7 - CONCLUSIONS

In this work, we have modeled a high-temperature/high-pressure desulfuration process (HTHPD) that employs a regenerable Zn/Ti based sorbent. The model is based on strongly simplified reaction kinetics, on proper black-box schematization of the known phenomenological aspects of the problem, on published data about process schemes and on the few available experimental results.

Then, the regenerative HTHPD model was embedded successfully into an existing process simulator, CAMEL, and integrated into a ZECOMIX plant model. The latter had been previously developed in the course of an independent project. The resulting process scheme is more complete, and allows for much more realistic and insight-generating simulations.

Creating the desulfuration reactor model was the most original part of this study. It relates the reactor performance with the sorbent characteristics and the operating conditions: temperature, pressure, syngas mass flow, H_2S concentration, etc., deriving real-scale reactor results from lab-scale experimental results. The performance curves obtained for the HTHPD do not make explicit use of reaction kinetics, but in a way "embed" it in an integral sense, in the same way a compressor operating map "embeds" the local thermo-fluiddynamics of the flow.

As such, the general method described in this Report can be used to derive the performance maps of any chemical reactor, paving the way to a series of practical applications in the development of process simulators.

REFERENCES

Section 1: Introduction

[1.1] Report of the Intergovernmental Panel on Climate Change (IPCC): Solomon, S., Qin, D., Manning, M., Chen, Z., Marquis, M., Averyt, K.B., Tignor, M., and Miller, H.L., "IPCC, 2007: Climate Change 2007: The Physical Science Basis", *Cambridge University Press, Cambridge, United Kingdom and New York, NY, USA* (2007).

[1.2] The United Nations Framework Convention on Climate Change (UNFCCC) "Article 2: Objective", *convention retrieved on November 15, 2005*.

[1.3] United Nations Environment Programme, "Industrialized countries to cut greenhouse gas emissions by 5.2%", *press release retrieved on August 6, 2007*.

[1.4] Fells, A., Fells, I., Horlock, J., "Cutting greenhouse gas emissions – a pragmatic view", *The Chemical Engineer (TCE)* (2005).

[1.5] Biegalski, S., "Generation III and IV reactors", *lectures from ME 361E Nuclear Reactor Engineering, University of Texas at Austin* (2007).

Section 2: Description of the Plant

[2.1] Meyer, J., Eriksen, D., Glockner R., Orjasaeter B., "Hydrogen production by integrated reforming and CO_2 capture"; *1st European Hydrogen Conference* , Grenobe, France (2003).

[2.2] Calabrò, A., Fiorini, P., Girardi, G., Sciubba, E., "Exergy analysis of a CO_2 zero emission high efficiency plant", *Proceeding of the International Conference ECOS 2004*, Guanajuato, Mexico (2004).

[2.3] Australian Coal Industry, "CO_2 Capture and Storage", *Coal 21* (2007).

[2.4] Working Group III of the Intergovernmental Panel on Climate Change (IPCC): Metz, B., Davidson, O., de Coninck, H.C., Loos, M., Meyer, L.A., "IPCC, 2005: IPCC Special Report on Carbon Dioxide Capture and Storage.", *Cambridge University*
Press, Cambridge, United Kingdom and New York, NY, USA (2005).

[2.5] University of California, Irvine, "Gasification", *National Fuel Cell Research Center Tutorials* (2007).

[2.6] Corrado A., Fiorini P., Sciubba E., "Environmental assessment and extended exergy analysis of a zero CO_2 emission, high-efficiency steam power plant", *Energy*, Volume 31, Issue 15 (2006).

[2.7] Turk, B.S., Merkel, T., Lopez-Ortiz A., Gupta, R.P., Portzer, J.W., "Novel technologies for gaseous contaminants control", *U.S .Department of Energy (DOE)* (2001).

Section 3: Sulfur Oxides

[3.1] U.S. Environmental Protection Agency (EPA), "Six Common Air Pollutants" (2007).

[3.2] The European Parliament and the Council of The European Union, "Directive 2001/80/EC", *Journal of The European Communities* (2001).

[3.3] Turk, B.S., Merkel, T., Lopez-Ortiz A., Gupta, R.P., Portzer, J.W., "Novel technologies for gaseous contaminants control", *U.S .Department of Energy (DOE)* (2001).

[3.4] U.S. Environmental Protection Agency (EPA), "Air Toxics" (2007).

[3.5] U.S. Environmental Protection Agency (EPA), "Air Pollution Control Technology Fact Sheet" (2003).

[3.6] U.S. Environmental Protection Agency (EPA), "Lesson 9. Flue Gas Desulfurization (Acid Gas Removal) Systems", SI 412C Course, Air Pollution Training Institute (APTI) Virtual Classroom (1998).

[3.7] SugarUdyoug.com, "Wet Scrubber, Controlling air pollution" (2007)

[3.8] Lozano Serrano, M.A., "Tema 6. Centrales termoeléctricas", *lectures from Tecnología Energética, University of Zaragoza* (2005).

[3.9] U.S. Environmental Protection Agency (EPA), "Lesson 7. Dry Scubbring Systems", SI 412C Course, Air Pollution Training Institute (APTI) Virtual Classroom (1998).

[3.10] Royo, J. "Tema 4. Sistemas aire-gases. Calderas de lecho fluido", lectures from Centrales Térmicas, University of Zaragoza (2005).

[3.11] U.S Department of Energy (DOE), "Fluidized Bed Technology", Clean Coal & Natural Gas Power Systems (2007).

[3.12] Energy Products of Idaho, "Fluidized Bed Combustion" (2007).

[3.13] Turk, B.S., Merkel, T., Lopez-Ortiz A., Gupta, R.P., Portzer, J.W., "Novel technologies for gaseous contaminants control", *U.S .Department of Energy (DOE)* (2001).

[3.14] GE Corporate Research and Development, "Enhanced Durability of High Temperature Desulfurization Sorbents for Moving-Bed Applications. Option 2 Program: Development and Testing Of Zinc Titanate Sorbents", *U.S Department of Energy (DOE)* (1993).

[3.15] Lew, S., Jothimurugesan, K., Flytzani-Stephanopoulos, M., "High-Temperature H_2S Removal from Fuel Gases by Regenerable Zinc Oxide-Titanium Dioxide Sorbents", *Ind. Eng. Chem. Res.*, Vol. 28, No. 5 (1989).
[3.16] Tamhankar, S.S., Bagajewlcz, M., Gavalas, G.R. "Mixed-Oxide Sorbents for High-Temperature Removal of Hydrogen Sulfide", *Ind. Eng. Chem. Res.*, Vol. 25, No. 2 (1986).
[3.17] Lew, S., Jothimurugesan, K., Flytzani-Stephanopoulos, M., "Sulfidation of Zinc Titanate and Zinc Oxide Solids", *Ind. Eng. Chem. Res.*, Vol. 31, No. 8 (1992).
[3.18] Konttinen, J.T., Zevenhoven, C.A.P., Hupa, M.M., "Hot Gas Desulfurization with Zinc Titanate Sorbents in a Fluidized Bed 1. Determination of Sorbent Particle Conversion Rate Model Parameters", *Ind. Eng. Chem. Res.*, Vol. 36, No. 6 (1997).
[3.19] Rutkowski, M.D., Klett, M.G., Zaharchuk, R., "Assessment of Hot Gas Contaminant Control", *Advanced Coal-Fired Power Systems '96 Review Meeting*, West Virginia, USA, on July 16, 1996.
[3.20] Turk, B., Schlather, J.,"Testing of a Warm-Gas Desulfurization Process in a Pilot-scale Transport Reactor System", *RTI International & Eastman Chemical Company*, *Gasification Technologies Conference, on October 4, 2006.*
[3.21] Portzer, J.W., Gangwal, S.K., "Bench-Scale Demonstration of Hot-Gas Desulfurization Technology", *Research Triangle Institute (RTI)* (1999).

Section 4: Physical Modeling

[4.1] Lew, S., Jothimurugesan, K., Flytzani-Stephanopoulos, M., "High-Temperature H_2S Removal from Fuel Gases by Regenerable Zinc Oxide-Titanium Dioxide Sorbents", *Ind. Eng. Chem. Res.*, Vol. 28, No. 5 (1989).
[4.2] Lew, S., Jothimurugesan, K., Flytzani-Stephanopoulos, M., "Sulfidation of Zinc Titanate and Zinc Oxide Solids", *Ind. Eng. Chem. Res.*, Vol. 31, No. 8 (1992).
[4.3] Turk, B.S., Merkel, T., Lopez-Ortiz A., Gupta, R.P., Portzer, J.W., "Novel technologies for gaseous contaminants control", *U.S .Department of Energy (DOE)* (2001).
[4.4] Turk, B., Schlather, J., "Testing of a Warm-Gas Desulfurization Process in a Pilot-scale Transport Reactor System", *RTI International & Eastman Chemical Company*, *Gasification Technologies Conference, on October 4, 2006.*
[4.5] Turk, B., Schlather, J.,"Testing of a Warm-Gas Desulfurization Process in a Pilot-scale Transport Reactor System", *RTI International & Eastman Chemical Company*, *Gasification Technologies Conference, on October 4, 2006.*
[4.6] Konttinen, J.T., Zevenhoven, C.A.P., Hupa, M.M., "Hot Gas Desulfurization with Zinc Titanate Sorbents in a Fluidized Bed 1. Determination of Sorbent Particle Conversion Rate Model Parameters", *Ind. Eng. Chem. Res.*, Vol. 36, No. 6 (1997).
[4.7] Konttinen, J.T., Zevenhoven, C.A.P., Hupa, M.M., "Hot Gas Desulfurization with Zinc Titanate Sorbents in a Fluidized Bed 2. Reactor Model", *Ind. Eng. Chem. Res.*, Vol. 36, No. 6 (1997).
[4.8] Chase et al., "JANAF Thermochemical Tables", *Journal of Physical and Chemical Reference Data*, Vol. 14 (1985).
[4.9] Konttinen, J.T., Zevenhoven, C.A.P., Hupa, M.M., "Modeling of Sulfided Zinc Titanate Regeneration in a Fluided-Bed Reactor 1. Determination of the Solid Conversion Rate Model Parameters", *Ind. Eng. Chem. Res.*, Vol. 36, No. 12 (1997).
[4.10] Konttinen, J.T., Zevenhoven, C.A.P., Hupa, M.M., "Modeling of Sulfided Zinc Titanate Regeneration in a Fluided-Bed Reactor 2. Scale-Up of the Solid Conversion Model", *Ind. Eng. Chem. Res.*, Vol. 36, No. 12 (1997).
[4.11] Portzer, J.W., Turk, B.S., Gangwal, S.K., "Durability Testing of the Direct Sulfur Recovery Process", *Research Triangle Institute (RTI)* (1996).
[4.12] Portzer, J.W., Gangwal, S.K., "Bench-Scale Demonstration of Hot-Gas Desulfurization Technology", *Research Triangle Institute (RTI)* (1999).
[4.13] Box, P., Gangwal, S., Weber, A., Howe, G., Potzer, J., Schlather, J., "Pilot Scale Demonstration of Direct Sulfur Recovery Process", *Research Triangle Institute (RTI)* (2005).

NOMENCLATURE

C	concentration of reactant gas (H_2S) [mol/m^3]
D_e	effective diffusion coefficient [m^2/s]
D_{e0}	frequency factor of diffusion coefficient [m^2/s]
E_a	activation energy of chemical reaction [kJ/mol]
E_d	activation energy of intrapellet diffusion [kJ/mol]
Eff	desulfurization efficiency [-]
Eff_{Reg}	regeneration efficiency [-]
ex	specific exergy [kJ/kg]
ExD	destroyed exergy [kW]
ExEff	exergetic efficiency [-]
Gi	input air stream
G(x)	conversion function defined by Eq. 8
h_f	specific enthalpy of formation [kJ/kg]
h	specific enthalpy [kJ/kg]
k_s	apparent chemical reaction rate constant [m/s]
k_{s0}	frequency factor of chemical reaction rate [m/s]
m_i	mass flow [kg/s]
m_{sorb}	amount of sorbent in the reactor [kg]
Mw_i	component i molecular weight [kg/kmol]
n_{S0}	flow of input reactant gas (H_2S) [mol/s]
n_{Zn}	total amount of zinc in the fluidized bed [mol]
N	total number of vertical slices in series
pi	flow i pressure [kPa]
p_r	reactor pressure [kPa]
p_{ref}	reference pressure [kPa]
P(x)	conversion function defined by Eq. 9
Qi	input heat [kW]
Q_l	parameter to determine lost heat [-]
Qlost	lost heat [kW]
R	universal gas constant (8.314 [J/mol/K])
R_0	sorbent pellet radius [m]
s	specific entropy [kJ/kg/K]
Si	input syngas stream
So	output syngas stream
t	time [s]
T_i	flow i temperature [K]
T_r	reactor temperature [K]
T_{ref}	reference temperature [K]
x	fractional sorbent conversion
x_i	component i weight fraction [-]
x_l	x at which the reaction control process changes
z_i	fraction of inlet sulfur captures into the ith slice
Zi	input sorbent stream
Zo	ouput sorbent stream
ρ	concentration of ZnO in sorbent [mol/m^3]
τ_1	constant defined by Eq. 10 [s]
τ_2	constant defined by Eq. 11 [s]

LIST OF ACRONYMS AND ABBREVATIONS

CAMEL: calculation by modular elements.
CCS: dioxide carbon capture and storage.
CHP: combined heat and power plants.
DSRP: Direct Sulfur Recovery Process.
ENEA: Italian National Agency for New Technologies, Energy and Environment.
FBC: fluidized bed combustion.
IGCC: integrated gasification combined cycle power plants.
IPCC: Intergovernmental Panel on Climate Change.
MEA: mono ethanol amine.
PM: particulate matter.
PPMV: parts per million by volume.
RHGD: regenerable hot gas desulfurization.
RTI: Research Triangle Institute.
TGA: thermo gravimetric analyzer.
VOCs: volatile organic compounds.
ZECOMIX: Zero Emission Coal Mixed.
ZECOTECH: Zero Emission Combustion Technology.